Channeling of fast particles and associated phenomena

V. A. Bazylev and N. K. Zhevago

I. V. Kurchatov Institute of Atomic Energy, Moscow
Usp. Fiz. Nauk **160**, 47–90 (December 1990)

The current state of the theory and experimentation in the field of interaction of relativistic electrons, positrons, and quanta of different energies with crystals in which the effect of channeling of particles plays an important role is reviewed. For relatively low energies, main attention is paid to effects of broadening of the spectral lines of emission in transitions between the levels of the transverse energy of the charged particles in the averaged field of the rows or planes of the crystal. The problem is studied on the basis of a theory that takes account of the deviation of the true potential of the crystal from the averaged potential of the rows or planes. In the region of medium energies ($\lesssim 10$ GeV) the main topic of the review is the stability of channeling, which reduces to the existence of integrals of motion in the averaged potentials. This problem is discussed in connection with the efficiency of conversion of the energy of the charged particles into energy of directional emission. In the region of high energies ($\gtrsim 10$ GeV), the review analyzes the various approaches in the theory of emission and formation of electron-positron pairs by photons in the field of the rows and planes of the crystal. A special place in the review is taken by a discussion of the possibility of channeling of quanta and neutrons in superlattices. Similarities and substantial differences are shown between this effect and the effect of channeling of charged particles of relatively low energies in crystals.

INTRODUCTION

Interest in the problem of channeling of electrons and positrons in crystals was given a boost in the mid-seventies in connection with the effect of electromagnetic radiation by particles during channeling, although even earlier a number of interesting results had been obtained in this field (see, e.g., Sec. 5 in Ref. 2). The number of publications on this theme in the scientific literature has hereafter steadily grown. This has been facilitated both by the practical interest attached to the use of the generated radiation and by the multifaceted character of the problem from the theoretical standpoint. We can provisionally distinguish three energy regions of channeled particles in which the character of their interaction with the crystal lattice and the character of the radiation substantially differ. In the region of low energies (< 100 MeV), quantum effects of the interaction of the particles with the crystal lattice are essential. In the region of higher energies ~ 1 GeV the character of the motion of the particles gradually becomes classical. Finally, at high energies $\gtrsim 10$ GeV, quantum effects in the radiation prove to be substantial.

In the low-energy region, at the initial stage of development of the theory, the mere possibility of observing radiative transitions between the levels of the transverse motion was discussed, and methods were developed mainly of calculating these levels in ideal crystals. In the region of medium and high energies of the emission from channeled particles, estimates were made primarily from the standpoint of applying it as a source of γ-quanta. However, at the early stage of the studies due attention was not paid to the effect of the stability of channeling on the intensity of emission. A certain stage in the development of theory and experiment in this field was reflected in the reviews[4,5,76] and monographs.[6,82] However, subsequently a considerable number of experiments was performed for varied crystals, including imperfect ones, at different particle energies. This has led to appreciable progress in the understanding the subtler mechanisms of interaction of particles with a crystal.

It turned out that the emission spectra of low-energy particles are sensitive to characteristics of the crystal such as the amplitude of thermal vibrations and the form factor of the atoms, the density of defects, the isotopic composition, and other very important properties of the crystals. These experiments have stimulated further development of the quantum theory of channeling that takes account of the deviation of the true lattice potential from the potential averaged over the crystal rows or planes, which is used, following Lindhard, as the first approximation of channeling theory. The energy of the particles employed in recent channeling experiments has been extended into the region of superhigh energies ≈ 150 GeV. At these energies a process was discovered of formation of channeled and superbarrier electron-positron pairs by a photon entering near row directions of the crystal. For these conditions, in which quantum effects in emission become dominant, the pertinent theory of emission and photon-pair formation in the field of the crystal rows and planes has been developed. Recently also a theory of the stability of channeled particles of medium and high energies has been intensively developed. This has permitted a more correct estimate of the possibility of emission in channeling as a source of gamma quanta for nuclear physics and elementary-particle physics. Finally, the problem of channeling of neutral particles, such as x-ray photons and thermal neutrons, has been studied quite recently.

A large number of interesting physical results obtained recently make it pertinent to review the problems discussed above. Indeed, we should note that some of the cited problems have been discussed quite recently in the review literature by other authors.[140–142] Reference 140 briefly reviews the current experimental literature on the spectroscopy of the states of channeled particles of low energy, but without the due theoretical analysis of the experimental results. Reference 142 discussed mainly the constant-field approximation in the theoretical analysis of possible polarization effects in emission and pair formation at high particle energies. A more complete treatment of the problem of emission and

 0038-5670/90/121021-26$01.00

pair formation has been conducted[141] within the framework of a quasiclassical operator method developed by the authors.

However, problems such as the theory of stability of channeling, the theory of broadening of spectral lines of emission by low-energy particles, as well as channeling of neutral particles, remained outside the scope of these reviews. On the other hand, the rather detailed theoretical analysis of the problem of emission and pair formation at high energies conducted in Ref. 141 was based entirely on the operator quasiclassical approach, and took no account of the existing alternative approaches.

In this regard this review is devoted mainly to the problems that were not presented, or were insufficiently presented in Refs. 140–142. In particular, in Sec. 1 of our review we present a theory of broadening of spectral lines of the emission from channeled particles that enables an analysis of the experimental results with account taken of the influence of the thermal lattice vibrations, the correlation of the thermal vibrations, the atomic form factors, and of crystal defects on the emission spectra. Section 2 discusses the theory of the stability of channeled particles of medium and high energies and analyzes the prospects of the emission from channeled particles as a source of γ-quanta. Section 3 presents the results of an alternative approach to the problem of emission and pair formation at high energies, based on the quantum theory of transitions between states of the transverse motion. The final Sec. 4 is devoted to a new phenomenon, the channeling of neutral particles. (The system of units with $\hbar = m = c = 1$ is used).

1. X-RAY SPECTROSCOPY OF THE QUANTUM STATES OF CHANNELED ELECTRONS IN CRYSTALS

1.1. Specifics of the channeling of electrons ($E \lesssim 100$ MeV)

As is known, the channeling of particles is the motion in the potentials of the atoms of rows or planes of a crystal averaged over the longitudinal coordinates (channels).[1-6] The difference between channeling of negative (e^-) and positive (e^+) charged particles consists in the fact that the atoms of a row (or plane) lie in the middle of the channel for e^- particles, rather than on its edges. Therefore the ordinary mechanism responsible for the suppression of scattering and stability of channeling of e^+ particles, which is associated with the inattainability of the small distances to the vibrating nuclei of the crystal, does not operate for e^- particles in the bottom of the well. Moreover, as the e^- particles approach a state of equilibrium, the perturbation does not decline as it does for e^+, but increases.

Nevertheless, even the first calculations of the experiments on the passage[7] and emission of electrons with energies $E \lesssim 50$ MeV[8,9] in light crystals revealed explicitly marked signs of channeling: transverse energy levels in the well of the averaged potential. The physical mechanism of the stability of quantum channeling of electrons was elucidated in Refs. 10 and 11 (see also Ref. 6). It consists in the following. When there is a small number $N \sim 1$ of levels in the channel, the transverse de Broglie wavelength $\lambda_D^\perp$ of an electron proves to be substantially larger than the amplitude u of the thermal vibrations of the atoms of the crystal. Thus it is impossible to localize the electron near a row or plane where it "senses" only an isolated atom. The blurring of the channeled electron leads to suppression of scattering by a factor of $(u/\lambda_D^\perp)^2$ as compared with the scattering by an isolated atom, despite the fact that the electron intersects the row or plane. Naturally, with increasing number of levels in the channel, i.e., with decreasing $\lambda_D^\perp$, the stated mechanism of stability disappears. This occurs with increasing energy of the electron or with increasing change of the nuclei of the crystal. For example, in crystals of gold and tungsten the instability of channeling can increase to the absolute amount.[10-13]

The development of experimental studies[14-35] of the discrete emission spectra associated with spontaneous radiative transitions between levels in a channel,[36] after the first studies,[8,9] has followed both the path of extending the energy range, orientation, and types of crystals, and of increasing the accuracy of determining the positions and widths of the observed x-ray emission lines. The problem of the theory consists in elucidating the influence of the characteristics of the crystal on the position, shape, and intensity of the emission lines.

1.2. Perturbation theory in channeling

The spectroscopic problem is attractive also because its solution can be based, not on modeling concepts, but on rigorous perturbation theory[10,11] in the deviation of the true operator for the interaction of the channeled particles with phonons and with the electronic subsystem of the crystal from the operator having conserved transverse energy in the channel. It is also important that the physical quantities that can be naturally calculated in the various orders of this perturbation theory are directly associated with those observable experimentally. Thus, in the zero-order approximation one can determine the transverse energy levels (strictly speaking, bands, since the channels are arranged periodically) and the corresponding wave functions[37,38] as the eigenvalues and eigenfunctions of the operator having the transverse energy conserved[39] (for more details see Ref. 6). In the following approximations one can determine the shifts and widths of the levels due to inelastic scattering of the channeled particles by the thermal vibrations of the lattice[10-12,40-42] and by the electrons[23,41,42] of the crystal. Further, one can study the shape of the emission lines, as well as the probability of transitions between the levels (bands).[10,11,42] By using the latter one can study the kinetics of population of the levels, i.e., the intensities of the individual emission lines.

A method convenient in practice of solving the problem for the eigenfunctions and eigenvalues in the zero-order approximation is that of expanding these functions and potentials of the channels in a series in the reciprocal-lattice vectors.[8] Here, instead of a second-order differential equation, we must solve a system of m algebraic equations. The number of these must be large enough that the energy band structure goes over into a continuous spectrum with a quadratic dependence of the transverse energy on the quasimomentum. Figure 1 shows the averaged potential of some planes of the silicon crystal, the energy levels in the channels, and the square of the wave functions of an electron of 4-MeV energy as calculated by this method.[17] Figure 2 shows the band structure of the entire spectrum of transverse energies having different quasimomenta in the bands as a function of the

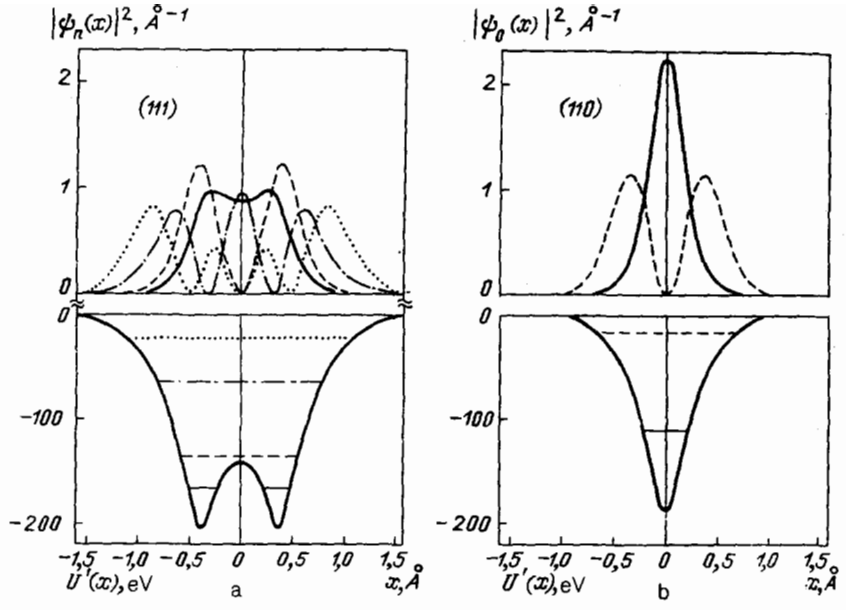

FIG. 1. The potential $U'(x) = \gamma U(x)$, where γ is the Lorentz factor, the energy levels of transverse motion in a coordinate system where the longitudinal velocity of the electron is zero, and the density of the distribution $|\psi_n(x)|^2$ of electrons of energy 4 MeV in (111) (a) and (110) channels (b) of silicon as a function of the distance from the plane.[17]

angle of entry of the electron into the crystal. It turns out in practice that 30 terms of the expansion suffice to attain the accuracy needed for spectroscopic purposes in the planar case, even at relatively high energies, 50 MeV.[12-22,24,43-46,50] In the row case the needed number of terms is large, ~900, which creates considerable computational difficulties.

To simplify the calculations, one can use the method of completely orthogonalized plane waves (the formalism of the pseudopotential; see, e.g., Ref. 52), which consists in the following as applied to the given problem.[53] The deeplying subbarrier states, whose band broadening is small, are calculated in the strong-coupling approximation. Here one can restrict the treatment to a single well of the transverse motion upon replacing the Bloch boundary conditions with conditions that the wave functions and their derivatives should vanish at infinity. The near-barrier and superbarrier states are calculated by using additionally introduced plane waves orthogonal to those found in the strong-coupling approximation. To avoid overfilling the basis of the number of supplementarily introduced Bloch functions (otherwise the finding of the widths is hindered or the accuracy is impaired), one subtracts a number of waves equal to the number of strong-coupled states. The details of applying the pseudopotential formalism in problems of row channeling, which enable one to decrease the rank of the matrices of the secular equation by more than an order of magnitude, can be found in Refs. 13, 41, and 53. Figures 3 and 4 show, e.g., the potential of a channel thus calculated, the square of the radial wave functions of the bound states in the channel, and the energy band structure of electrons of energies of 3.5 MeV, 4 MeV, and 5 MeV in different row channels of silicon.

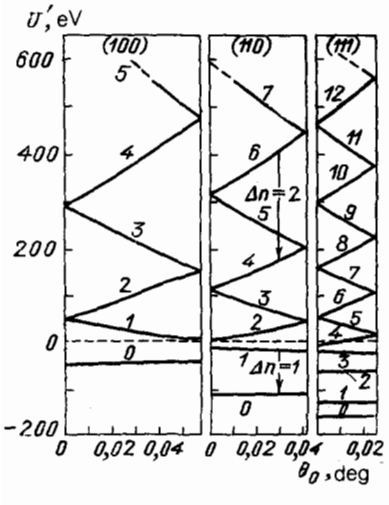

FIG. 2. Band structure of the spectrum of energies of transverse motion (in a system of longitudinal rest of an electron of 4-MeV energy) with different quasimomenta in the bands[17] as a function of the angle of entry of the electron into the crystal with respect to the (100), (110), and (111) planes of silicon.

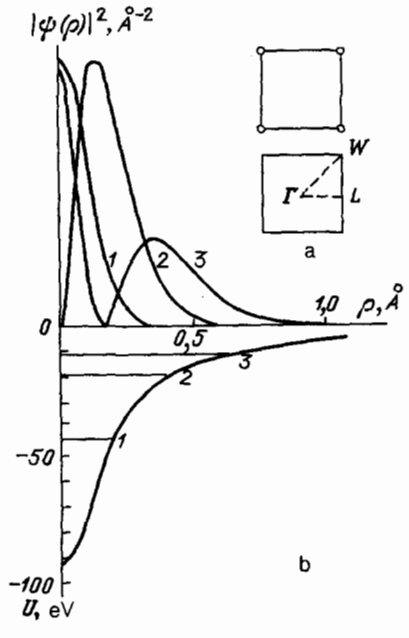

FIG. 3. Unit cell and first Brillouin zone (a), the potential (b), and density of the radial distribution (in the direction of L) of electrons of 5-MeV energy on the ⟨100⟩ row of silicon in different bound states.[53]

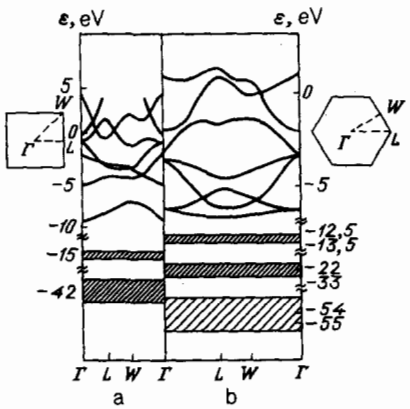

FIG. 4. Energy band structure in row channeling of electrons of 3.5-MeV energy in the ⟨100⟩ channel (a) and of 4 MeV in the ⟨111⟩ channel (b) of silicon.[13]

The cellular method has been used in a number of studies[143,144] to calculate the band structure of the energy levels of the transverse energy of particles in planar channeling. In this approach the problem is reduced to solving the Schrödinger equation with the relativistic mass inside one cell of the periodic potential of the planes having the boundary conditions

$$\psi(d/2) = \exp(i\varkappa d)\psi(-d/2),$$
$$\psi'(d/2) = \exp(i\varkappa d)\psi'(-d/2)$$

that relate the wave functions and their derivatives at the boundaries of the one-dimensional cell. On the basis of this method, algorithms were developed[143] that enable one to find the spectrum of transverse energies $\varepsilon_n(\varkappa)$ as a function of the transverse quasimomentum $\varkappa$ of the particles, as well as the wave functions and matrix elements of the radiative transitions between the bands.

We should note that the listed approaches to the problem of the band structure of transverse energies are in essence one-dimensional or two-dimensional (in the row case) analogs of the known approximations used in the theory of the electronic structure of solids.

1.3. Dependence of the position of the emission lines on the characteristics of the crystal

As was pointed out in Refs. 17 and 54, the position of the emission lines is highly sensitive to the details of the distribution of the electron density in the crystal. Thus, in Ref. 17 the energy levels in the channels were calculated for different models of the electron-density distribution in the isolated atom. The approximations of Moliere[55] and of Doyle and Turner[56] for the atomic potential were used. The calculations showed (Table I) that the Doyle and Turner approximation yields values closest to the experimental positions of the emission lines, but it also does not lead to complete agreement with experiment. Consequently the authors of Ref. 17 concluded that the atomic form factors are satisfactorily approximated in Ref. 56 only for relatively small transferred momenta $q \lesssim 2$ Å^{-1}, and obtained an improved approximation for $q \lesssim 6$ Å^{-1}. The improved approximation of the form factors led to 2% agreement in the positions of the lines with experiment for the (100) and (110) planes and the ⟨100⟩ row of the diamond crystal for various electron energies (Fig. 5 and Table II). The authors of Ref. 48 were able to improve the accuracy of the calculations to 1%. At the same time, for the case of the doubled ⟨110⟩ rows and (111) planes of the diamondlike lattice, the asymmetric distribution of electron density around an atom of the crystal owing to the covalent bonds of the atoms becomes essential. The position of the levels proves to be sensitive to this effect. Actually the studies that have been performed in these cases have shown very significant deviations of the experimental data from the theory that uses the form factors of the isolated atom (Fig. 6). Attention was turned in Ref. 25 to the need to take account of the deviation of the electron distribution in the crystal from a spherically symmetric distribution. A treatment taking account of this difference while using the experimental data on x-ray diffraction by the (111) plane brought the theoretical and experimental values of the positions of the lines closer. However, appreciable discrepancies (5%) yet remained, which exceed the error of experiment and theory (see Fig. 6). Thus the x-ray diffraction data did not allow reaching full agreement of theory and experiment. More accurate data on the asymmetry of the electron distribution might be obtained upon more accurate measurement of the intensity of the high-order reflections (third-order, etc.) in x-ray diffraction. However, this study has not yet been carried out. At the same time, the spectroscopy of the x-ray emission in channeling is already at the attained level of accuracy in a position to fix the disagreement of experiment and the existing views on the details of the electron distribution in the crystal (see Fig. 6). As a result of such comparisons the authors of Ref. 33 started with the agreement of the theoretical and experimental data on the position of the emission lines, and concluded that one must introduce cor-

TABLE I. Position of the emission lines ω_{if} in planar channeling ((110) direction) of electrons in silicon.[17]

E, MeV	Transition i–f	Experiment: ω_{if}^{max}, keV	Theory: ω_{if}^{max}, keV	
			Moliere approximation	Doyle–Turner approximation
56	1—0	128	139	134
	2—1	94	101	96
	3—2	68	75	69
	4—3	52	58	53
28	1—0	40	45	43
	2—1	25	28	27

TABLE II. Position of the emission lines ω_{if} in channeling of electrons in diamond.[33]

Indices of plane (or row)	E, MeV	Transition i–f	Experiment: ω_{if}^{max}, keV	Theory: ω_{if}^{max}, keV
(110)	54,5	1—0	161,0±0,5	163,7
		2—1	103,8±0,4	105,7
		3—2	78,0±0,3	79,6
		4—3	60,3±1,5	59,7
		4—1	240,2±1,5	245,0
⟨100⟩	16,9		101,5±1,0	100,0
			58,3±0,5	57,9
			35,0±0,5	33,9

rections to the potential of the (111) plane that take account of the deviation of the electron distribution from spherically symmetric.

The temperature of the crystal, and hence also the amplitude of the thermal vibrations of the atoms, as was first noted in Ref. 12, also exert an appreciable influence on the position of the emission lines in channeling, especially those involving radiative transitions to the deepest levels. Figure 7 shows the influence of the temperature of the crystal on the form of the potential of the channel, the position of the levels in the channel, and the observed emission spectra of electrons of 54.4-MeV energy.[35] With the given distribution of the electron density in the crystal, the position of the hardest emission lines, which involve transitions to the deep levels, prove to be highly sensitive to the amplitude of the thermal vibrations, and hence to the Debye temperature. Thus, the authors of Refs. 34 and 35, while studying the emission spectra of electrons in crystals of Cd, Si, Ge, and GaAs (Table III), concluded that the Debye temperature in silicon, obtained from experiments on channeling, proves to be appreciably lower than the generally accepted value (540 K), in contrast to the situation for diamond and gallium arsenide. Figure 8 shows the measured and the calculated positions of the emission lines for plane and row channeling for two different Debye temperatures θ_D.[34,35] We see that $\theta_D = 493$ K best describes the experimental situation. However, we should note that, strictly speaking, an entire class exists of distribution functions of the electron density of the crystal and intervals of the corresponding Debye temperatures for which one can attain in principle an agreement of the theo-

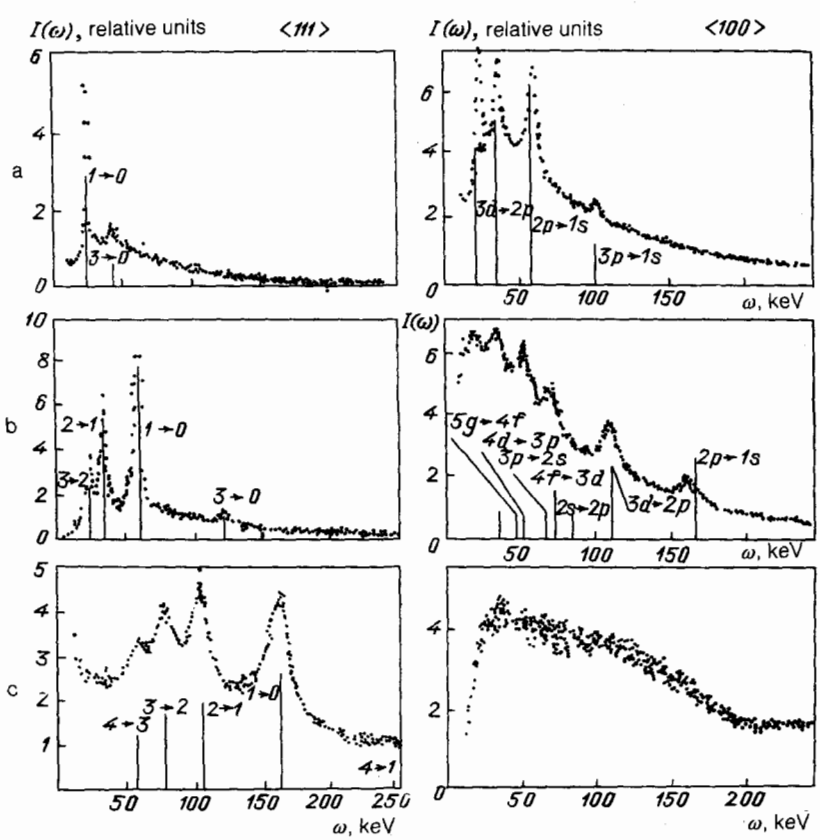

FIG. 5. Spectra of the emission intensity of (111) planar (left) and ⟨100⟩ row (right) channels in diamond for different electron energies (in MeV): 16.9 (a), 30.5 (b), and 54.5 (c).[33] Solid lines–calculated values of the centers of emission lines (see Table II).

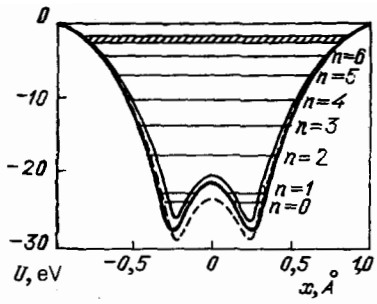

FIG. 6. Potential of the (111) channel of diamond and energy levels of transverse motion in the channel for 30.5-MeV electrons. Dashed line–potential obtained from the Doyle-Turner approximation of the potential of an isolated atom; thin solid line–potential obtained from experiments on x-ray diffraction; thick solid line–potential obtained from the condition of coincidence of the experimental and theoretical values of the positions of the emission lines[33] (x–distance from the plane).

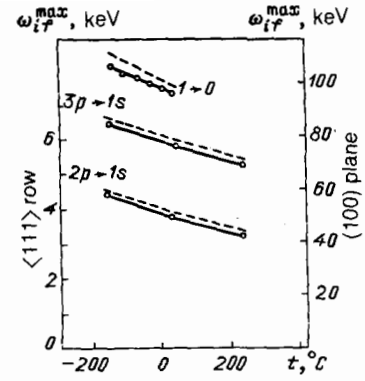

FIG. 8. Measured (symbols)[24,34,35] and calculated (curves)[34,35] positions of emission lines in the 3p→1s and 2p→1s transitions of electrons of 3.5-MeV energy in the ⟨111⟩ row channel and of the 1→0 transition in the (100) planar channel of silicon at an energy of 54.5 MeV of electrons as functions of the temperature of the crystal. The solid lines correspond to a Debye temperature of 495 K, the dashed lines to 543 K.

retical and experimental data. Therefore, to obtain an accurate value of θ_D, one must fix the electron-density distribution as accurately as possible. Such a study has been performed in Refs. 47 and 48. To approximate the electron-density distribution found in Ref. 17, they obtained $\theta_D = 514$ K (for $T = 110$ K), and $\theta_D = 504$ K (for $T = 298$ K). For a more exact approximation,[48] the values obtained were $\theta_D = 503$ K (for $T = 110$ K), and $\theta_D = 494$ K (for $T = 298$ K).

The results of precision measurements of the positions of the emission lines in channeling of electrons in crystals of LiF, LiH, and LiD proved to be interesting.

Thus, the authors of Refs. 29 and 31 concluded that the amplitude of the thermal vibrations of the fluorine atoms in the LiF crystal is decreased by a factor of almost two, while the amplitude of the thermal vibrations in the LiH crystal is larger than in LiD, in contradiction to the previously known result.[57] Actually this conclusion follows directly from comparing the emission spectra (Fig. 9), since, with identical lattices, the increase in the amplitude of thermal vibrations is accompanied by a shift in the emission line toward lower frequencies (which is the more appreciable for harder emission lines), while their intensity declines.

Studies of the influence of crystal imperfections on the position of emission lines in channeling have certain prospects owing to two circumstances: one can study the relatively deep layers of a crystal (~ 1 μm); the discrete structure of the emission spectrum is manifested even with a large amount of damage and dislocations;[31] the position, shape, and intensity of the emission lines are highly sensitive to the existing crystal imperfections. Figure 10 shows the results of an experiment[31] to measure the emission spectrum of electrons in channeling in a perfect crystal (dots) and in an imperfect crystal with a given density of dislocations (circles). As the experiment implies, a fully regular influence exists on the emission spectra: a shift into the soft region, broadening, and intensity decrease of the emission lines–laws that beg for theoretical description. The now evolving theory of the influence of crystal imperfections on the emission spectra explains these laws[51] and makes it possible to extract information on certain characteristics of the crystal imperfections (e.g., dislocations in type-B diamond).

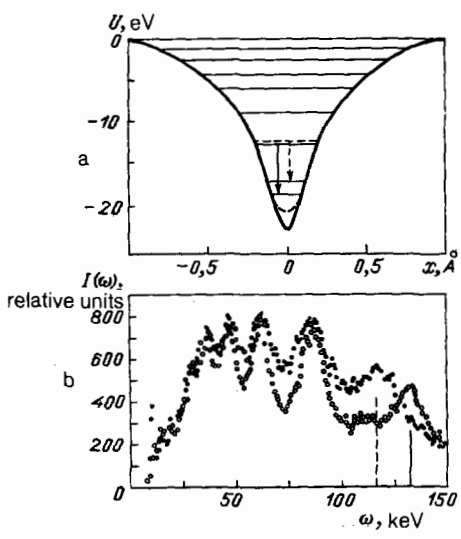

FIG. 7. a–Potential of the (110) planar channel of silicon and positions of the transverse energy levels in the channel for 54.5-MeV electrons for two different temperatures: 80 K (solid lines), and 293 K (dashed lines). b–Emission spectra of 54.5-MeV electrons in the (110) channel of silicon at 80 K (solid dots) and 293 K (light circles).[35]

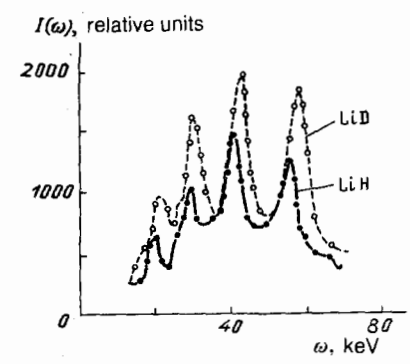

FIG. 9. Emission spectra of electrons of energy 54.5 MeV in the (100) planar channel of LiH and LiD crystals.

TABLE III. Position of emission lines associated with the $1 \to 0$ transition in different crystals for the given Debye temperature θ_D.[34]

Crystal	E, Mev	θ_D, K	$\omega_{1\to0}^{max}$, keV: plane (110)	
			Theory	Experiment
Cd	54,4	2000	163,7	161±0,5
Si	54,4	543	128,5	122,2±1,0
Ge	16,9	290	26,9	27,6±0,5
GaAs	16,9	260	26,6	26,6±0,4

As is known, an overwhelming fraction of natural diamond single crystals have a high (up to 10%) concentration of a nitrogen impurity whose presence in the lattice leads to the formation of disks. Dislocations of this type, as studied by x-ray diffraction and electron microscopy, lie chaotically and have dimensions from 40 to 1000 Å. Two models are known of the incorporation of disks into the diamond lattice.[44,51] According to one of them, the dislocation constitutes a double disk made of nitrogen atoms; according to the other–a single disk of carbon atoms. However, the existing experimental methods do not yield exhaustive information on these dislocations. At the same time, the first, albeit insufficient (for details see Sec. 1.4), data from measurements of the positions of emission lines in imperfect crystals[31] lead to some quite definite conclusions. Thus, it was shown[51] that the concept of dislocations as consisting of a single disk of carbon atoms is closer to the real situation in experiment; the diameter of the disks is ≈ 200 Å, while the density of disks is $\approx 3\times10^{10}$ cm^{-2}. The distance between the disks was assumed to be known ($\Delta \approx 500$ Å[31]). The conclusions on the structure of the dislocations were made from the condition of coincidence of the theoretical and experimental values of the positions of emission lines for two electron energies in planar channeling. For the case of rows (there are no experimental data), which can yield additional information (see Sec. 1.4), the calculations are given in Table IV.

It is of definite interest to study the influence of point isomorphous defects (substitution) on the position and width of emission lines in channeling. The corresponding theory has been developed in Ref. 44. Table V shows the results of such calculations for Si without dopants ($q \leqslant 0.1\%$), with a 1% and 5% boron doping (p-type silicon), and with 1% and 5% arsenic doping (n-type silicon). As the Table implies, point isomorphous defects shift the emission lines by an amount sufficient for experimental detection at a defect concentration $q \geqslant 1\%$.

1.4. Influence of the characteristics of the crystal on the width and intensity of the emission lines in channeling

The width Γ_i of a level is composed of the band width $\Gamma_i^{(b)}$ and the widths due to inelastic scattering by the phonons, $\Gamma_i^{(n)}$, and electrons, $\Gamma_i^{(e)}$, of the crystal. For planar channeling there also exists a specific inhomogeneous broadening, $\Gamma_i^{(s)}$ involving the Doppler effect in the scattering of the particles in the plane of channeling,[11] since different particles emit photons of different frequencies in a given direction. Naturally, for spectroscopic studies of the homogeneous broadening of the shape of an emission line that depends on the details of the electron-density distribution ($\Gamma^{(e)}$, $\Gamma^{(b)}$) and of the thermal vibrations ($\Gamma^{(n)}$), the stated inhomogeneous broadening is a "blurring" effect.

In Ref. 46 all of the processes cited above of line broadening of emission lines of channeled electrons in diamond were calculated. Table VI gives the results of the calculations together with the experimental values.[21] As the Table implies, a considerable contribution to the width of the emission lines comes from the Doppler broadening due to scattering of the particles in the plane of the channel (up to 50% of the total width and often considerably exceeding the broadening due to thermal vibrations).

The band broadening, as implied by Table VI, is substantial for the high-lying levels; in a number of cases, e.g., in the (100) plane, it can become decisive. The calculations performed in Ref. 46 show also that the calculated and experimental data agree only upon taking account of the quantum effect pointed out above of scattering suppression[10,11] due to the periodic arrangement of the atoms.

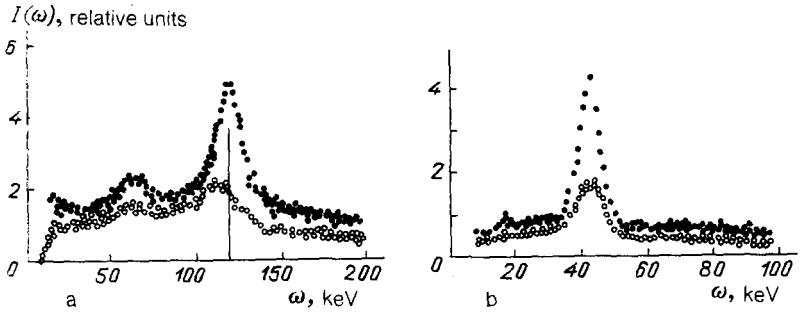

FIG. 10. Measured emission spectra of electrons of energy 54.5 MeV (a) and 30.5 MeV (b) in the (100) planar channel of diamond of different degrees of perfection.[31]

TABLE IV. Position ε_i, shift $\Delta\varepsilon_i$, width Γ_i in a perfect crystal, and dislocation width Γ_i^g of levels in the ⟨100⟩ row channel for electrons of different energies E for two models of dislocations.[44,51]

E, MeV	Level	ε_i (Γ_i), eV	$\Delta\varepsilon_i$ (Γ_i^g), eV	
			Model 1	Model 2
5	1s	—41,4 (0,41)	—1,23 (0,24)	—1,30 (0,24)
	2p	—17,0 (0,25)	—0,47 (0,06)	—0,56 (0,064)
16,9	1s	—57,8 (0,47)	—1,63 (0,36)	—1,70 (0,37)
	2p	—34,6 (0,38)	—1,10 (0,16)	—1,17 (0,19)
	2s	—24,0 (0,24)	—0,69 (0,10)	—0,77 (0,11)
	3s	—19,5 (0,23)	—0,60 (0,069)	—0,68 (0,074)
	3p	—16,3 (0,27)	—0,41 (0,066)	—0,50 (0,068)
30,5	1s	—64,9 (0,45)	—1,78 (0,41)	—1,84 (0,42)
	2p	—44,4 (0,47)	—1,37 (0,27)	—1,44 (0,27)
	2s	—32,1 (0,28)	—0,96 (0,16)	—1,05 (0,17)
	3s	—28,6 (0,32)	—0,93 (0,14)	—1,01 (0,14)
	3p	—23,7 (0,25)	—0,67 (0,10)	—0,77 (0,11)

TABLE V. Position of emission lines of channeled electrons in silicon doped with boron (p) and arsenic (n)[44] (q is the concentration of the dopant).

Miller indices	E, MeV	Transition	$\omega_{if}^{(0)}$ keV, $q \leqslant 0.1\%$	$\omega_{if}^{(p)}$ keV, 1%	$\omega_{if}^{(p)}$ keV, 5%	$\omega_{if}^{(n)}$ keV, 1%	$\omega_{if}^{(n)}$ keV, 5%
⟨100⟩	3,5	2p→1s	3,25	3,27	3,36	3,21	3,06
(110)	54	1→0	125,2	125,7	127,7	124,2	120,4

TABLE VI. Measured[21] and calculated[46] line widths Γ of the emission in planar channeling of electrons of energy 54 MeV in diamond.

Miller indices	Transition i–f	$\Gamma^{(n)} + \Gamma^{(e)}$ keV	$\Gamma^{(b)}$ keV	$\Gamma^{(g)}$ keV	Γ_{theor} keV	Γ_{exp} keV
(110)	1→0	4,3	—	5,1	9,4	12,1
	2→1	3,8	—	3,3	7,1	8,7
	3→2	3,4	0,4	2,5	6,3	7,6
	4→3	3,0	4,6	1,8	9,4	8,8
(100)	1→0	3,1	0,9	4,1	8,1	8,0
	2→1	2,2	12,5	3,7	18,4	24,0

TABLE VII. Partial widths Γ of levels in ⟨100⟩ and ⟨111⟩ row channels of silicon for electrons of energies 3.5 and 4 MeV.[13]

States	Si, $E = 3.5$ MeV; ⟨100⟩			Si, $E = 3.5$ MeV; ⟨111⟩		
	$\Gamma^{(n)}$, eV	$\Gamma^{(e)}$, eV	$\Gamma^{(b)}$, eV	$\Gamma^{(n)}$, eV	$\Gamma^{(e)}$, eV	$\Gamma^{(b)}$, eV
1s	300	25	<1	478	35	<1
2p	79	19	<1	170	31	<1
2s	30	16	320	70	30	<1
3d	10	6	350	20	8	235

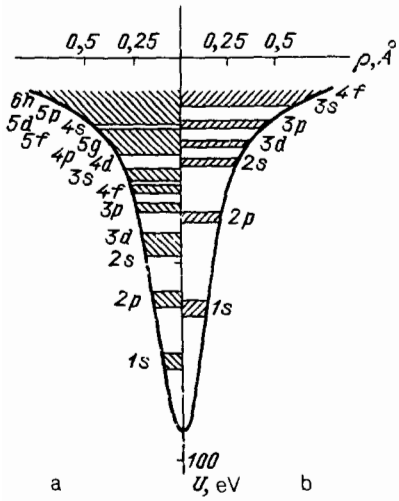

FIG. 11. Broadening of levels in a row channel of Si of electrons of energies 50 MeV (a) and 15 MeV (b).[13]

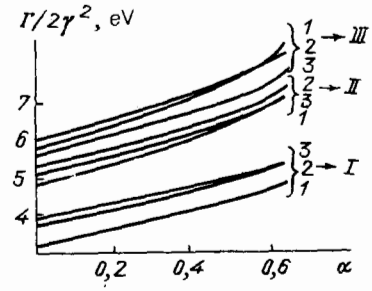

FIG. 12. Dependence of the width of the 2p→1s emission line on the correlation coefficient of the thermal displacements of the silicon atoms for electrons in the ⟨100⟩ channel with energies of 3.5 MeV (curves *I*), 7.5 MeV (curves *II*), and 11.5 MeV (curves *III*) for different crystal temperatures: 100 K (*1*), 300 K (*2*), 500 K (*3*).

Row channeling offers certain prospects from the standpoint of obtaining information on the crystal by using the widths of the emission lines. The advantage over the planar case consists in absence of a Doppler broadening that blurs the effect, while the band broadening is substantially smaller than in the planar case. Consequently, scattering by phonons predominates for the deep levels, and that by electrons for the outer levels. Table VII and Fig. 11 show illustrative data.[13]

The influence of crystal imperfections on the widths of the emission lines has been treated in Refs. 44 and 51 within the framework of the above-mentioned perturbation theory in the deviation of the interaction operator of a channeled electron with the real crystal from the operator with conserved transverse energy in an ideal crystal. The results of these studies imply that the absolute values of the dislocation widths amount to 20–50% of the values of the widths in a perfect crystal for the real dislocations of natural diamond, while various models of the dislocations give rise to a small difference in the values of the dislocation widths (see Table VI). We note that, by using the experimental values of the widths and positions of the emission lines in several row orientations and values of the electron energy, one can obtain data on the density, dimensions, and structure of the dislocations without fixing their parameters.

As regards point isomorphous defects, the widths of the levels in Si are very sensitive to doping with atoms having a large atomic number. This can be seen from Table VIII for Si doped with boron and arsenic. This situation can prove essential in obtaining information on semiconductor materials of high conductivity.

As is known, no methods exist for direct measurement of the correlation coefficients of the thermal displacements of the atoms of a crystal lattice. In particular, one of the methods currently most popular, EXAFS, allows one to measure the difference in magnitudes of the mean squares of the relative displacements of the atoms at different temperatures, and with an accuracy of $\sim 10\%$.[59,60] At the same time, as was shown in Ref. 41 (see also Ref. 12), one can obtain more accurate, and in a number of cases even direct, information on the magnitudes of the correlation coefficients by studying the widths of hard emission lines in row channeling. Figure 12 shows, e.g., the calculated dependence of the widths with different energies in a row channel of silicon on the magnitude of the correlation coefficient α at different temperatures The contribution from inelastic scattering by electrons to the width of the emission lines amounts in this case to 2%. As we see from the graph, we have $\Gamma \approx \Gamma_0(1+\alpha)$. For the known values of α (see Refs. 61–63) the correction to the width from correlations in the thermal displacements reaches 20–30%. Table IX shows the measured[24] widths of the emission lines in the 2p→1s transitions of electrons of energy 3.5 MeV in Si (⟨111⟩ direction) at temperatures of 110, 300, and 500 K and the values calculated in Ref. 41 of the widths without taking account of correlations, and with taking account of them in the Debye model with α from Ref. 63. As the Table implies, taking account of correlations according to the Debye model yields an increased value of the width. One can determine the correlation coefficients between the different neighbors from the condition that the theoretical widths should agree with the experimental values.[41] We should bear in mind that, in situations in which the correlations between different pairs of

TABLE VIII. Width of the lowest transverse-energy level of channeled electrons in pure ($q<0.1\%$) silicon and silicon doped with boron (p) and arsenic (n) (E–energy of the electrons, q–concentration of dopants.

Miller indices	E, MeV	Γ, eV $q<0.1\%$	Γ, eV 1%	Γ, eV 5%	Γ, eV 1%	Γ, eV 5%
⟨100⟩	3,5	1,79	1,77	1,68	1,89	2,29
⟨110⟩	54	0,311	0,300	0,289	0,325	0,382

TABLE IX. Width of the (2p→1s) emission line in ⟨111⟩ row channel of silicon calculated[41] without taking account of correlations (Γ_1), with account taken of correlations by the Debye model (Γ_2), and by the model of Ref. 63 (Γ_3) at different temperatures (Γ_{exp}–experimental value of the line width.[24]

T, K	Γ_{exp}, eV	Γ_1, eV	Γ_2, eV	Γ_3, eV
110	530	400	640	480
300	650	465	790	610
500	670	485	800	625

atoms in the row are substantial, one cannot directly determine the corresponding correlation coefficient by comparing theory and experiment. In such cases one must base the treatment on some concrete model of the correlations.

The intensity of the emission lines depends on the populations C_i of the quantum states in the channel. In turn, the populations depend on the thickness of the crystal, the angle of emergence, and the rate of dechanneling (the probabilities of transition between states and the widths of the levels). For example, by varying the angle of entry, one can enhance, or vice versa, suppress individual emission lines. To illustrate this situation, Fig. 13 shows the dependences of the emission spectra in the ⟨111⟩ row channel of silicon on the angle of entry with respect to the row. The capabilities of x-ray spectroscopy will appreciably increase if we learn, when comparing theory with experiment, to work with several more parameters: the absolute intensities of the different emission lines. To do this in the theory we must solve the balance equation, and in setting up the experiment we must have well calibrated detectors with high resolution. This problem has already been solved in Refs. 21, 23, and 46. The degree of agreement of theory and experiment, which was not bad for the initial stage of studies, is a stimulus for further spectroscopic studies.

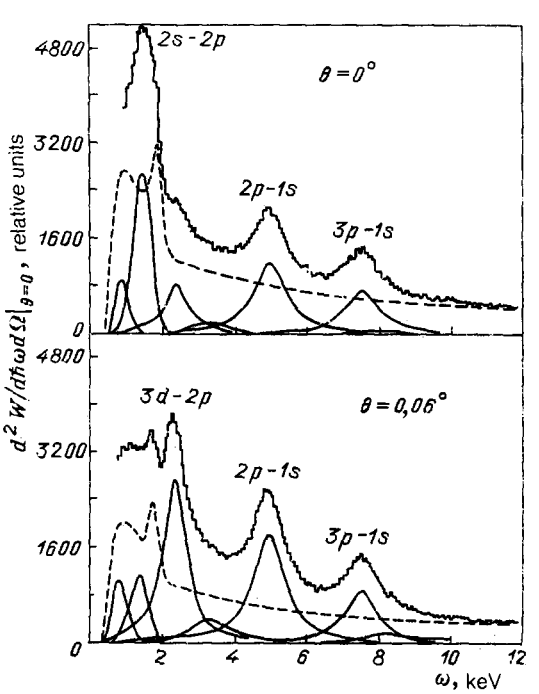

FIG. 13. Measured emission spectra (broken lines)[12] of 4-MeV electrons in the ⟨111⟩ row channel of silicon 0.5-μm thick for two different entry angles: $\theta = 0°$–upper diagram, $\theta = 0.06°$–lower diagram; dashed curve–spectrum in a disoriented crystal with account taken of absorption of photons; solid curves–theoretical interpretation of the contribution of individual transitions.

The ratio Δ_{if}/Γ (Δ_{if} is the spacing between the levels) decreases[10,11] with increasing energy of the electron (Fig. 12). Crossing of the levels implies, on the one hand, that the possibility of applying x-ray spectroscopy vanishes (see also Fig. 5). On the other hand, it implies that the widths of the levels cease to be an adequate characteristic of the process. However, since the number of levels here proves to be even larger, the classical description holds.

2. SCATTERING, DECHANNELING, AND ENERGY LOSSES OF ELECTRONS IN CRYSTALS AT HIGH ENERGIES

2.1. Scattering of electrons in oriented crystals

If the number of discrete levels in the well of the averaged potential $U(r_\perp)$ of depth U_0 and width a is large enough ($a(EU_0)^{1/2} \gg 1$, see Ref. 6), then the condition of classical motion of an electron having a total energy E is satisfied. We shall characterize the scattering by the mean square of the angle of deflection $\langle\theta_d^2\rangle$ of the particle from its initial direction. In studying the scattering of an electron in a crystal, it is convenient to distinguish three different mechanisms: coherent scattering by the averaged potential of the rows and planes; scattering accompanied by exchange between the electron and the crystal (as a whole) of a momentum that is a multiple of the reciprocal-lattice momentum; and finally, incoherent scattering by the thermal vibrations of the atoms of the crystal lattice. The cited mechanisms contribute additively to the mean square of the angle of deflection $\langle\theta_d^2\rangle$ of the electron from the initial direction.

In scattering by the averaged potential $U(r_\perp)$, a channeled electron is deflected over the path length $z \approx d/\theta_L$ by an angle of the order of the Lindhard angle $\theta_L \approx (2U_0/E)^{1/2}$ (in the row case the angle of deflection is several times smaller than θ_L owing to the funnel-shaped form of the potential of a row channel). Here d is the distance between the atoms. With increasing angle of entry θ_0 with respect to the row or plane, the angle of deflection decreases. Thus, for the case of a plane we have $\langle\theta_d^2\rangle = (\Delta U/E\theta_0)^2$, where $\Delta U = U(r_\perp^0) - U(r_\perp^f)$, Here $r_\perp^0$ and $r_\perp^f$ are the coordinates of the point of entry (and emergence), which are random quantities, as we can easily convince ourselves upon using the condition of invariance of the transverse velocity in passing through the boundary of the crystal. In the row case a rotation of the velocity vector of the crystal about the row by

the angle φ also occurs under the action of the averaged potential, where we have $\langle\theta_d^2\rangle = \theta_0^2\langle\varphi^2\rangle$. In thin crystals ($z \leqslant d^2/a\theta_0$), when the particle can be scattered only by one chain, the phenomenon of rainbow scattering can occur,[64,65] which is analogous to the phenomenon of rainbow scattering of waves and particles by water drops, atoms, and atomic nuclei. The effect involves the coherent addition of scattering amplitudes at the same angle for different angular momenta of the particle with respect to the crystal row. At relatively great thicknesses $z > d^2/a\theta_0$, multiple scattering by the chains will occur, for which the deviation from the initial direction will accumulate owing to the mean-square angle $\langle\varphi^2\rangle$ of scattering by the different chains of the crystal.[66,67] This angle can be calculated analytically by using the Born theory of scattering by a two-dimensional Lindhard potential.[4] Consequently, the following formula was obtained in Refs. 4 and 66 for the mean-square angle of deviation:

$$\langle\theta_d^2\rangle = \frac{\sqrt{3}\,(4-\pi)\cdot 4\pi^2 Z^2 e^4 naz}{E^2 d\theta_0}. \tag{2.1}$$

Here Z is the nuclear charge of the atoms of the crystal, d is the distance between the atoms in a chain, a is the Thomas–Fermi screening radius, and e is the charge of an electron. This angle, just like the "single"-scattering angle by a plane or chain, at small entry angles $\theta_0 \ll 1$ can substantially exceed the multiple-scattering angle in an amorphous material. The factor by which it exceeds, which is equal in order of magnitude to $a/d\theta_0$, coincides with the coherence factor, which increases the scattering and emission cross section in the crystal as calculated per isolated atom.[4] At great enough thicknesses of the crystal $z \gtrsim d^2\theta_0^3/a\theta_L^4$, for which the azimuthal angle $\langle\varphi^2\rangle$ approaches unity in order of magnitude, the mean-square angle of deviation $\langle\theta_d^2\rangle$ approaches saturation (characteristic annular distributions are formed (see, e.g., Ref. 68), as observed in experiments with well collimated beams of protons and π-mesons[69]).

Practically always, one need not take account of the coherent scattering involving the periodic discreteness of the row or plane, in line with the low probability of transfer of such a large longitudinal momentum as the reciprocal-lattice momentum. The mechanism being discussed is important only in the regime of transition from planar channeling to row channeling (then the transferred momentum approaches zero), since precisely this mechanism makes necessary the replacement of the zero-order approximation (replacement of the planar continuous potential by the sum of the row potentials).[6]

For sufficiently large thicknesses $z \gg d/\theta_L$ (for $\theta < \theta_L$) and $z \gg d^2\theta_0^3/a\theta_L^4$ (for $\theta_0 > \theta_L$), for which the coherent scattering reaches saturation, we must take account of the incoherent scattering involving the thermal vibrations of the atoms of the crystal.[70,145]

Since at high electron energies the incoherent scattering is from a single isolated atom (see below), the deviation of the mean-square angle of scattering by the thermal vibrations of the atoms in the crystal from the analogous quantity in an amorphous target (or a disoriented crystal) involves only the effect of redistribution of the electron flux over the cross section of the channel.

When $\theta_0 > \theta_L$, one can derive an analytic formula for the redistribution of the electron flux, and hence, for the ratio of the mean square of the angle of scattering $\langle\theta^2\rangle_T$ by the thermal vibrations of the atoms in the planar channel to the mean square of the scattering angle in an amorphous target $\langle\theta^2\rangle_a$ by starting with a concrete model of the averaged potential of the planar channel. For example, for the model of an "inverted parabola," the stated ratio is:[70]

$$\frac{\langle\theta^2\rangle_T}{\langle\theta^2\rangle_a} = 1 - \frac{\theta_L^2}{3\theta_0^2}. \tag{2.2}$$

As is implied by (2.2), the scattering of superbarrier particles in the crystal by the thermal vibrations of the atoms is barely weaker than the scattering in a disoriented crystal. The effect becomes more appreciable as the entry angle θ_0 approaches the critical channeling angle θ_L, which involves the "hovering" of the electrons lying immediately near the barrier in the region of reduced nuclear density. The maximal deviation from $\langle\theta^2\rangle_a$ is of the order of 10%.

When $\theta_0 < \theta_L$, the effect of flux redistribution has no rigorous analytic expression, even for concrete models of the potential of the channel; however, for qualitative description of the effect one can use the approximate formula:[70]

$$\frac{\langle\theta^2\rangle_T}{\langle\theta^2\rangle_a} = 1 + \frac{\alpha U_0}{\varepsilon_{max}(z)}\left(1 - \frac{1}{6\alpha}\ln\frac{\varepsilon_{max}(z)}{U_0}\right); \tag{2.3}$$

Here U_0 is the total depth of the well for the planar channel, α is a parameter of the order of unity, $\varepsilon_{max}(z) = E\langle\theta^2\rangle_a(z)/2$, $E_s \approx 21$ MeV, L is the radiation length, and

$$\langle\theta^2\rangle_a = \frac{E_s^2 z}{E^2 L}\left(1 + \frac{1}{9}\lg\frac{z}{L}\right). \tag{2.4}$$

As Eq. (2.3) implies, if all the particles lie in the channel ($\varepsilon_{max}(z) \leqslant U_0$), then the scattering by the thermal vibrations at small entry angles of the electron into the crystal ($\theta_0 \ll \theta_L$) is several times more intense than the scattering in a disoriented crystal. This is quite natural, since the channeled electrons on the average move in a region of elevated nuclear density in the crystal. For large thicknesses the quantity $\langle\theta^2\rangle_T$ approaches the analogous quantity $\langle\theta^2\rangle_a$ in an equivalent amorphous target from the low side, owing to the contribution of the superbarrier particles, while differing from $\langle\theta^2\rangle_a$ by no more than 10–20%[70] (see also Eq. (2.2)).

We note that direct measurement of the angle of multiple scattering by the thermal vibrations $\langle\theta^2\rangle_T^{1/2}$ in channeling is possible only in a thick enough crystal, since the angles of multiple scattering by the averaged potentials of the planes and rows prove to be substantially smaller than $\langle\theta^2\rangle_T^{1/2}$ owing to the saturation effect. However, as was shown in Refs. 70 and 145, these angles in a thin crystal can be measured indirectly by using the intensity of the hard component of the incoherent emission spectrum. The stated component of the spectrum arises from the bremsstrahlung of the electron by the vibrating nuclei of the crystal, while the intensity of this emission in the absence of collimation of the photon beam is proportional to $\langle\theta^2\rangle_T$.

Thus the overall pattern of the evolution of the scattering with the thickness of the crystal must take account of all the examined mechanisms. For example, in the case of row orientation, even with zero entry angle of the electrons with respect to the axis of the crystal, an accurate calculation must take into account at first the scattering by the continuous potential in the channel, and then the multiple scatter-

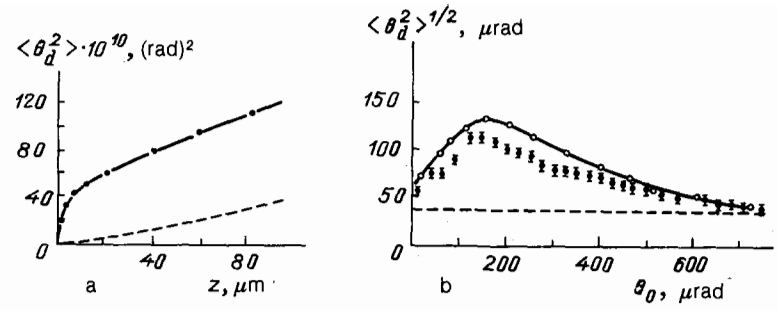

FIG. 14. a–Mean square of the angle of scattering of 10-GeV electrons in silicon at an entry angle of the electrons of $\theta_0 = 30$ μrad with respect to the ⟨111⟩ row as a function of the thickness of the crystal. The dotted curve corresponds to an amorphous target. b–Orientational dependence of the scattering angle of 10-GeV electrons in a silicon crystal (⟨111⟩ row) 40-μm thick. Solid dots–experiment,[68] open circles with solid envelope–calculation by the computer-simulation method,[58] dashed line–calculation for an amorphous target.

ing by the chains of the superbarrier electrons that have arisen as a result of incoherent scattering by the thermal vibrations. Here the incoherent scattering starts out first as the mechanism of "feeding" of the superbarrier states, and only then (in thick crystals) as the fundamental mechanism of angular broadening of the beam.

Figure 14a shows the total mean square of the scattering angle of electrons of energy 10 GeV in a silicon crystal calculated by computer simulation[58] for an entry angle of the electrons $\theta_0 = 30$ microradians with respect to the ⟨111⟩ row ($\theta_L = 140$ microradians) as a function of the thickness of the crystal. As the diagram implies, the mean square of the scattering angle in an amorphous target (dotted line) is substantially smaller than the analogous quantity in a crystal. Figure 14b shows the theoretical and experimental orientational dependence of the scattering angle of 10-GeV electrons at different entry angles with respect to ⟨111⟩ into a silicon crystal 40-μm thick.[68] The diagram shows rather good agreement of theory and experiment.

We should note that an increase in the scattering angles in crystals in row orientation as compared with an amorphous medium has been observed at energies $E \lesssim 1$ GeV as early as in the 70s at Khar'kov.[86] Later more detailed studies of this problem were performed there.[87]

2.2. Dechanneling. Limits of applicability of the adiabatic approximation

In contrast to the coherent scattering by the averaged potential of the rows and planes of the crystal, the incoherent scattering by the thermal vibrations of the atoms, which was discussed in Sec. 2.1, does not conserve the energy ε of transverse motion. Here, for negatively charged particles in the bottom of the well of the averaged potential, the physical mechanisms for suppression of scattering that are responsible for justifying the distinction between the superbarrier and channeled fractions and the stability of channeling disappear. Moreover, it turned out that the mean square of the angle of scattering of channeled electrons by the thermal lattice vibrations appreciably exceeds the mean square of the angle of scattering of the superbarrier electrons (see Eq. (2.3) for a thickness z_ε of the order of the period of oscillations in the channel d/θ_L and (2.2)). Consequently, for electrons with energy $E \gtrsim 100$ MeV, one must study the possible existence of regions of absolute instability of channeling. The most rigorous and consistent solution of this problem must be based on analyzing the kinetic coefficients obtained within the framework of perturbation theory from the deviation of the true interaction operator of the channeled electron with the phonons and electrons of the crystal from the averaged operator.[71] These coefficients D_k have the form:[6,71]

$$D_k = \lim_{l\to\infty} \sum_f W_{if} (\varepsilon_i - \varepsilon_f)^k \quad (k = 1,2). \tag{2.5}$$

Here the W_{if} are the probabilities of transition between different states in the channel, while $\lim_{l\to\infty}$ denotes going over to classical wave packets consisting of a rather large number of close-lying quantum states. The coefficients D_1 and D_2 respectively denote the mean increment $\overline{\delta\varepsilon}$ and the mean-square fluctuation $(\overline{\delta\varepsilon^2})^{1/2}$ of the transverse energy ε in the period of motion of the particle in the channel. The coefficients obtained thus, for which we can find expressions in Refs. 6 and 71, contain as limiting cases both the case of the unattainability of small distances to the nuclei (dechanneling by the fluctuations of the continuous potential), and the converse case of close collisions, in which scattering by an isolated atom occurs. At the same time they describe the intermediate region, as is specifically characteristic of row channeling of electrons.

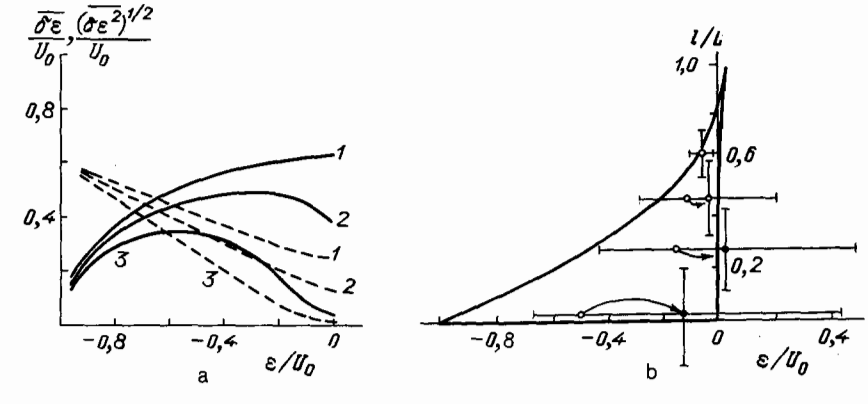

FIG. 15. a–Dependence of the mean increment $\overline{\delta\varepsilon}$ (dashed lines) and the mean-square fluctuation $(\overline{\delta\varepsilon^2})^{1/2}$ (solid lines) of the transverse energy on ε for different values of the angular momentum of the electrons with respect to the ⟨111⟩ row of silicon. *1* corresponds to zero angular momentum, *2* to an angular momentum equal to half the maximum possible (for the given ε), *3* to the maximum possible angular momentum. $L = 50\hbar$, $U_0 = 100$ eV is the depth of the well. Energy of the electrons is 1 GeV. b–Region of bound motion in the space of the transverse energy ε and the angular momentum l for the case of row channeling of electrons of 1-GeV energy about the ⟨111⟩ row of silicon. The open circles show the parameters (ε, l) for several electrons an the entrance to the crystal; the crosses demonstrate the variation ("drift" and "spread") of the initial parameters during one revolution about the row.

Figure 15a, which shows the values of $\overline{\delta\varepsilon}$ and $(\overline{\delta\varepsilon^2})^{1/2}$ calculated in Ref. 71 for the ⟨111⟩ axis channel in Si at an electron energy of 1 GeV, illustrates the fact that the fluctuation of the transverse energy

$$\max\left\{\frac{\overline{\delta\varepsilon}}{\varepsilon},\ \frac{(\overline{\delta\varepsilon^2})^{1/2}}{\varepsilon}\right\}$$

is larger than (or of the order of) unity when $E \lesssim 1$ GeV. For the sake of graphic description, Fig. 15b shows arbitrarily the evolution of the "probability cloud" in the space of the energy ε and the angular momentum l (the region associated with the row of motion is bounded by the heavy lines). We see that, in the time of one revolution around the row, any point inside the region can spread by an amount comparable with the distance to the boundaries of the region. The fact that the adiabaticity parameter $\delta\varepsilon/\varepsilon$ can become comparable with or greater than unity throughout the depth of the well implies not only the failure of the transverse energy ε as an integral of motion, but also the impossibility in the strict sense of distinguishing between channeled and superbarrier particles. For states of high angular momentum ($l \gg \hbar$) in a row channel, which initially are practically not scattered by the nuclei owing to their remoteness from them, this occurs via inelastic scattering by the electrons of the crystal. In a time of the order of the time of revolution around the row, an electron of energy $E \lesssim 1$ GeV either immediately goes over into the superbarrier region, since the binding energy of the high-angular-momentum states is small owing to the centrifugal term, or it goes into highly extended orbits with a rather small (for strong scattering by the nuclei of the row) minimal distance to the nuclei.[71] For the low-angular-momentum states of row channeling, and also states of planar channeling, the stated absolute instability stems from the following simple arguments. Let us estimate the ratio of the mean-square angle of scattering by the thermal vibrations in (2.3), built-up in the time of flight $z \sim d/\theta$ alongside the plane, to the angle $\theta = [2(\varepsilon - U_0)/E]^{1/2}$, at which the electron intersects the plane (or row), while assuming that the transverse energy is conserved, at least for a period of vibration:

$$\frac{\langle\theta^2\rangle_T^{1/2}}{\theta} \approx \frac{E_s d^{1/2}}{E^{1/4}(\varepsilon - U_0)^{3/4} L^{1/2}}. \tag{2.6}$$

This ratio also determines the ratio of the mean-square fluctuation of the transverse energy $(\overline{\delta\varepsilon^2})^{1/2}$ to ε over the period of the oscillations, while its square determines the ratio of the increment $\overline{\delta\varepsilon}$ to ε.[75] By using (2.6) one can easily find that the stated ratio is close to unity when $E \leqslant 1$ GeV, even for light crystals (of the type of diamond or silicon, $L \approx 10$ cm, $E_s \approx 21$ MeV, $d \approx 1$ Å). More rigorous treatment confirms this result for the planar[75] and row[71] cases. The ratio (2.6) depends weakly on the energy ($\sim E^{-1/4}$). Therefore the assumption of the existence of a transverse energy is justified only at high enough energies. An experimental confirmation of the effect of absolute instability of channeling of electrons of energy 50 MeV in a row channel has been obtained in Ref. 49.

Since an electron energy region exists where the transverse energy is not an adiabatic invariant of the motion, we must also change the approach to solving the kinetic problem. As is well known, the general Boltzmann kinetic equation

$$\frac{\partial f}{\partial z} + \mathbf{V}_\perp \nabla_\perp f + \mathbf{F}_\perp \frac{\partial f}{\partial \mathbf{p}_\perp} = \mathrm{St}\{f\} \tag{2.7}$$

allows simplification in two limiting cases.[79] In the case, known as the adiabatic approximation, of a sufficiently small collision integral St $\{f\}$, one can go from the general Boltzmann equation in the space of the transverse momenta and coordinates of the particles to an equation of smaller dimensionality in the space of the integrals of motion. Naturally, here the variation of the integrals of motion owing to collisions in a period must be relatively small ($\delta I \ll I_0$). As applied to the problem of channeling of protons, such an approach in kinetics was first used by Martynenko[72] (for more information see Refs. 73 and 74). In the other limiting case in which $\delta I \gg I_0$ (the collision integral is large), the so-called hydrodynamic approximation is known. As applied to channeling problems, this limit is not attained in practice, since here $\delta\varepsilon/\varepsilon \sim 1$, and then one must either solve the general Boltzmann kinetic equation or use the methods of computer simulation, as presented, e.g., in Ref. 58.

The stated situation is especially important in finding the spectral intensity of the emission from electrons. As is known, the emission spectrum of electrons of energies $E < E_c^{(1)}$ (see Table IX) is formed in a time much greater than the time of collision with one plane or row of the channel. Here the spectral distribution of the emission substantially depends on whether these collisions are correlated in time or not. The absence of transverse energy as an adiabatic invariant of motion can lead to transformation of the periodic trajectories into aperiodic ones, and thus, to a substantial change in the spectral distribution of the emission from the electrons. Strictly speaking, when $\delta\varepsilon/\varepsilon \sim 1$, the trajectories of the electrons are not determined by the averaged potential, while the spectral distribution of the emission is expressed in terms of the Fourier transform of the correlation function (see Ref. 6).

Akhiezer and Shul'ga[76] predicted the irregularity of the motion for an appreciable fraction of the electrons in a row channel, even in the absence of random collisions with the nuclei and electrons. The irregularity (stochasticity) of the motion in the case that they studied of electrons near the barrier, which lie in a region with negative curvature of the potential energy, is a consequence of the existence of one integral of motion in a system with two degrees of freedom.[77,78] This situation also substantially affects the spectral composition of the emission from the electrons.

At sufficiently large electron energies, one must take account of the reaction of the radiation on their motion in the channels of the crystal.[80-82] This effect is taken into account not only by the fact that the total energy E of the electron becomes a function of the thickness of the crystal, but also by the extra term in the kinetic coefficients D_k, which implies taking account of the influence of the losses of transverse energy on the motion in the channel:

$$D_1^{(\mathrm{rad})} = \frac{v_\perp^2}{2}\frac{\mathrm{d}E}{\mathrm{d}z}; \tag{2.8}$$

Here $D_1^{(\mathrm{rad})}$ is the local value of the losses of transverse energy described by Eq. (3.4) (see below), whose form is the same in the classical and quantum cases. The total losses with account taken of possible emission of hard photons

($\omega \sim E$) is described by the expression (see also Sec. 3):

$$\frac{dE}{dz} = e^2 f(\chi), \quad f(\chi) \approx \frac{2\chi^2}{3}, \qquad \chi \ll 1, \qquad \approx 0{,}82\chi^{2/3}, \quad \chi \gg 1, \tag{2.9}$$

where $\chi = E/E_c^{(2)}$ (Table X).

The fundamental contribution to the kinetic coefficients D_i in (2.5) comes from the region $r_\perp \sim u$. Therefore, to estimate the electron energies $E^{(\mathrm{rad})}$ at which the variation of the transverse energy due to emission becomes comparable with the corresponding quantity due to scattering, we can start with the condition of approximate equality of the local values of D_i (x) when $x \sim u$. As a result it turns out that $E^{(\mathrm{rad})}$ does not differ in order of magnitude from $E_c^{(2)}$ (see Table X) for different crystals and directions. When $E > E^{(\mathrm{rad})}$, the stability of the motion of the electrons in the channel increases owing to the decrease in ε. We note that $E \sim E^{(\mathrm{rad})}$ is practically the energy region in which the parameter χ becomes of the order of unity, i.e., the region of substantial quantum recoil. Since, when $E > E^{(\mathrm{rad})}$, the losses of longitudinal energy prove to be more substantial than the losses of transverse energy, the angular divergence of the beam increases.[80]

2.3. Angular density of the energy losses of electrons in emission with account taken of scattering in crystals of limiting thickness

The angular density of the emitted energy (the brilliance) is the most essential characteristic of γ-sources for purposes of high-energy physics. Therefore it is important to evaluate correctly the prospects of creating sources of high brilliance based on emission arising in the passage of ultrarelativistic electrons through oriented single crystals.

To attain the maximum energy fluxes, one should use crystals of the limiting thickness. The limiting thickness, as defined by the absorption of quanta in the crystal, reaches 0.1–0.2 radiation lengths.[83] An exact calculation of the characteristics of the emission in such thick crystals is difficult, owing to the need for solving the cumbersome kinetic problem of (2.7). The known simplification of the problem by going over to the kinetics of quasiparticles in transverse-energy space would merit attention as an estimate were it not for the remaining complexity and immensity of the solution. At the same time, in analyzing the experimental data, evaluating the prospects, and seeking possible pathways for optimizing the γ-source, numerical calculations lose to analytic calculations. Therefore, in presenting the problem of the brilliance of emission in oriented crystals, we shall follow Ref. 84, where a solvable analytic model was formulated, which enables one to estimate the intensity of emission of electrons in crystals of limiting thickness with satisfactory accuracy.

The fundamental idea that simplifies the treatment is based on the following two results:[70,71]

1) the mixing of states in the well of the averaged potential is so fast that it makes no sense to classify them into sub- and superbarrier fractions, while the distribution of the flux of electrons over the cross section of the "channel" in a thick crystal is close to uniform;

2) the average, over the flux, of the square of the angle of multiple scattering of the electrons in an oriented crystal of great thickness differs only in corrections from the analogous quantity in an amorphous target. Actually, these two results imply that the general Fokker–Planck equation in the space of transverse momenta and coordinates (see (2.7)) in a thick enough crystal can be solved by the method of successive approximations in the deviation of the distribution of electron fluxes in the "channel" from a uniform distribution. Here one uses in the zero-order iteration the values from (2.6) for the angle of multiple scattering and the corresponding zero-order distribution function over the transverse momenta and coordinates. Rigorous calculations of this type have not yet been performed. However, within the framework of this idea one can apply a model in which the processes of multiple scattering occur in the same way as in an amorphous substance, but rectilinear motion is strongly distorted by the action of the averaged potential. This model enables one to write and solve an approximate system of equations for the average, over the beam, of the angular energy density of emission $dE/d\Omega$ of the electrons in the oriented row of a crystal of limiting thickness:[84]

$$\frac{dE^{\mathrm{row}}}{d\Omega} = \frac{\alpha E_0^3}{\pi E_s^2}\left(1 + \frac{E_0}{E_A}\right)\ln\left\{1 + \frac{0{,}3E_s'^2}{[1+(E_0/E_A)][1+(E_0/E_B)]}\right\}. \tag{2.10}$$

Here E_0 is the initial energy of the electron, α is a coefficient of the order of unity, $d\Omega$ is the differential of the solid angle, and E_A and E_B are two characteristics of the energy that correspond to the choice of the crystal and orientation,

$$E_A = \frac{3S_0}{2\pi e^2 U_0^2 L}, \quad E_B = \frac{m^2}{2U_0}; \tag{2.11}$$

TABLE X. Values of the threshold energies $E_c^{(1)} = 1/U_0$, the critical energies $E_c^{(2)} = 1/(\nabla U)_{\max}$, and the critical entry angles $\theta_c = U_0$ of superbarrier particles for different crystals, rows, and planes and two temperature values: $T = 293$ K (upper values), $T = 100$ K (lower values).

293 K / 100 K	(110) Si	⟨110⟩ Si	(110) Ge	⟨110⟩ Ge	(110) W	⟨111⟩ W
$E_c^{(1)}$, GeV	12,3 / 11,6	2,4 / 1,9	8,0 / 7,1	1,4 / 1,0	2,25 / 2,1	0,28 / 0,22
$E_c^{(2)}$, GeV	1199 / 1018	144 / 95	702 / 545	86 / 47	156 / 129	12,6 / 7,5
$\theta_c \cdot 10^5$	4,16 / 4,42	21,1 / 26,8	6,4 / 7,16	37,7 / 53,2	22,7 / 24,3	180 / 232

TABLE XI. Values of the parameters E_A and r for some of the most frequently used crystals and orientations.[84]

Crystal	Cd ⟨110⟩	Cd (110)	Si ⟨110⟩	Si (110)	Ge ⟨110⟩	Ge (100)	⟨111⟩ W	(100) W
E_A, GeV	0,36	2,5	1,1	12	1,5	22	0,48	18
r	0,25	0,5	0,9	1,9	2,3	5,5	3,4	11

S_0 is the cross section of the "channel," U_0 is the depth of the well of the averaged potential, m is the mass of the electron, e is its charge, while $E_s' = 14$ MeV.

For an amorphous substance or a disoriented target one can use (2.10), where E_A, $E_B \to \infty$, while $U_0 = 0$. Consequently the following formula holds for the ratio of the angular densities of the emission energy in an oriented and a disoriented crystal:

$$f^{\text{row}} \equiv \frac{dE^{\text{row}}/d\Omega}{dE^{(a)}/d\Omega} = \frac{1+(E_0/E_A)}{5{,}44} \ln\left\{1 + \frac{0{,}3E_s'^2}{[1+(E_0/E_A)][1+(E_0/E_B)]}\right\}. \quad (2.12)$$

Formulas just as simple hold for a planar ($\theta_0 = 0$) orientation of the crystal.[84] The values of E_A and $r = E_A/E_B$ for certain rows and planes of the most common crystals are contained in Table XI.

Experimental studies of the angular density of radiation in crystals of limiting thickness were conducted with the Tomsk synchrotron[85] at an electron energy of 900 MeV and with different row orientations of diamond, silicon, and tungsten. Table XII gives the experimental values of the ratio f of the angular density of emission in an oriented crystal ($\theta_0 = 0$) to the analogous quantity in an amorphous target, as taken from Ref. 85, and the theoretical values of this quantity f calculated by Eq. (2.12). As the amorphous level, data were taken that were obtained for aluminum, and are presented (along with data for crystals) in Fig. 2 of the cited study.[85] As Table XII implies, the discrepancy of theory and experiment does not exceed the overall error of measurement.

Figure 16 shows (dashed curves) the variation of the quantity f for different values of the parameter $r = E_A/E_B$. An important feature of this variation is the existence of a maximum at a certain energy E_{opt} of the electrons. The magnitude of the ratio f^* at the maximum and the corresponding initial energy E_0^{opt} of the electrons are shown in Fig. 17 by the dashed lines. The analogous results for a plane[84] are shown in Figs. 16 and 17 by solid lines. With increasing energy $E > E_{\text{opt}}$, the ratio of the angular densities of radiation in a crystal and an amorphous target declines. The reason is that at these energies the total losses in the crystal become saturated. Hence they are about the same as in an amorphous target of limiting thickness ($\Delta E \sim E_0$), while the effective solid angles of emission in the crystal ($\Delta\Omega_{\text{eff}}^{(c)} \sim U/E$) become larger than the effective emission angles in an amorphous substance ($\Delta\Omega_{\text{eff}}^{(a)} \sim E_s^2/E_0^2$). We note that at large energies $E_0 > E_c^{(2)}$, owing to quantum recoil (see Sec. 3), the ratio of the angular densities declines even more rapidly, since the rate of total losses slackens off (see Eq. (2.12)).

Upon using the data of Table XII, we can easily convince ourselves, by using Fig. 17, that the maximum excess of f^* over the amorphous level is small and can reach values from 2 to 4, depending on the type of crystal. Since f^* declines with increasing r (Fig. 16), to create sources of maximum brilliance one should use crystals with small atomic number Z, for which the parameter r is minimal (see also Refs. 85–87).

3. THE INFLUENCE OF CHANNELING ON EMISSION AND ELECTRON-POSITRON PAIR FORMATION AT SUPERHIGH ENERGIES

3.1. The constant-field approximation

Channeled electrons and positrons, even of rather high energies (up to ~10 GeV) in crystals that are not too heavy, mainly emit photons whose energy ω is substantially smaller than the energy of the emitting particles.[4–6] The laws of conservation of energy and longitudinal momentum in emission in a field of planes or rows of a crystal lead[88] to a threshold energy of a channeled particle $E_c^{(1)} = 1/U_0$ (U_0 is the depth of the potential well, $\hbar = m = c = 1$) below which the emission of a photon of energy $\omega \approx E/2$ is impossible, even if the particle undergoes transition from the highest levels of transverse energy to the bottom of the potential well. At high energies one can employ a classical treatment of the motion

TABLE XII. Experimental[85] and theoretical[84] values of the ratio of the angular density of emission energy of oriented crystals of limiting thickness to the corresponding quantity in an amorphous target.

Crystal	Cd ⟨100⟩	Si ⟨111⟩	W ⟨111⟩
f_{exp}	2,5±0,2	1,7±0,2	1,3±0,1
f_{theor}	2,4	1,5	1,3

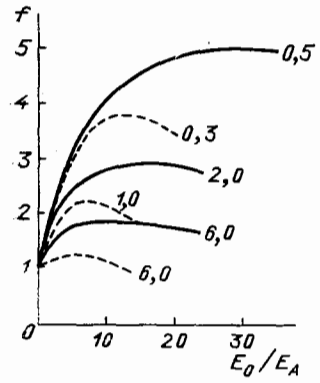

FIG. 16. Ratio f of the angular energy density of emission in an oriented crystal to the corresponding quantity in an amorphous target as a function of the ratio of the energy E_0 of the electrons to the energy E_A (see Table XI). The solid curves correspond to planar orientation, and the dotted curves to row orientation. The numbers on the curves show the values of the parameter $r = E_A/E_B$.

of the channeled particle. The energy $E_c^{(1)}$ corresponds to the condition of equality of the angle of deflection of the channeled particle by the field of planes or rows of the crystal, $\theta_d \approx (2U_0/E)^{1/2}$, to the effective emission angle $\theta_{eff} \approx 1/E$. At energies close to the threshold, the probability of emission of hard photons for which the parameter $u = \omega/(E-\omega)$ is larger than unity is relatively small. However, this probability increases rapidly with increasing ratio $E/E_c^{(1)}$.

At superhigh energies $E \gg E_c^{(1)}$ the angle of deflection of the particle by the field of the planes considerably exceeds the effective emission angle. This means that the radiation is formed in the relatively short coherence time $\tau_{coh} \sim u/E$, which is small in comparison with the interval between successive collisions of the particle with the rows or planes of the crystal. In this case the analysis of the emission process is substantially simplified, since we can consider the field acting on the particle to be constant in space within the limits of the short intervals of time of formation of the emission.

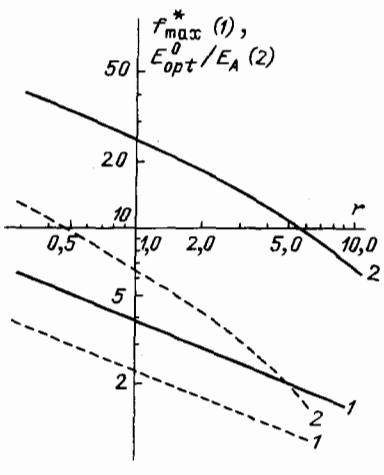

FIG. 17. Dependence on the parameter r of the maximum value f_{max} (curves *1*) and of the ratio of the initial energy $E_{opt}^{(0)}$ of the electrons corresponding to f_{max} to the energy E_A (*2*). The solid curves are drawn for the case of planes, and the dotted curves for rows.

Hence the emission spectrum must be analogous to the spectrum of magnetic bremsstrahlung in a constant field.[89–94] Within the framework of the constant-field approximation, the spectrum of the emission from a small region of the trajectory is completely determined by the acceleration of the particle, which depends in this case on the transverse coordinates (see, e.g., Ref. 95). The observed emission spectrum is obtained further by averaging over the time of motion along the trajectory, and also be averaging over all possible trajectories of the particles.[89,90] According to the classical theory,[6,89,90] the maximum of the spectrum lies at the frequencies $\omega \sim \omega_c = (3/2)E^2|\nabla U|$, where E is the energy of the particle, and ∇U is the gradient of the potential energy of the particle in the field of the rows or planes of the crystal. Hence we can find[96] the energy $E_c^{(2)} = 1/|\nabla U|$, at which the emission spectrum reaches the essentially quantum region $\omega \sim E$, and the classical treatment of the emission process loses force. In a reference frame moving together with the particle along the rows or planes, the field of the crystal looks like crossed electric $\mathscr{E}'$ and magnetic $\mathscr{H}'$ fields with the intensity $\mathscr{E}' = \mathscr{H}' = E|\nabla U|/e$, which is larger by a factor of $\gamma = E$ than the electric field intensity in the laboratory system (see, e.g., Ref. 5). Thus the critical energy $E_c^{(2)}$ has also the meaning that, when $E = E_c^{(2)}$, the field in the moving system becomes equal to the Schwinger field $\mathscr{H}_3 = m^2c^3/e\hbar = 4.41\cdot 10^{10}$ T ($\mathscr{E}_0 = 1.32\times 10^{18}$ V/m).

The maximum value of the gradient of the potential (i.e., the electric field) $|\nabla U|_{max}$ is reached at distances from the plane or row of the order of the radius of thermal vibrations of the atoms. Even if we take as the estimate of $E_c^{(2)}$ the maximum value of the electric field, the values of $E_c^{(2)}$ prove to be 30–50 times higher than the threshold energy $E_c^{(1)}$.[96] For the row case $E_c^{(2)}$ amounts to several tens, and for the planar case to several hundreds of GeV (see Table X). For particles that do not approach closely enough the rows or planes in channeling, the effective values of $E_c^{(2)}$ can be even higher, since the field intensity declines rapidly at distances from the row or plane greater than the radius of thermal vibrations. At superhigh energies $E \sim E_c^{(2)}$, we must take account of the recoil in the process of emitting a photon, as well as of the effects involving the existence of spins of the particles. The spectral distribution of the emission intensity with account taken of quantum effects in the constant-field approximation looks as follows (see, e.g., Ref. 97):

$$\frac{dW}{du} = \frac{e^2}{\pi\sqrt{3}}\frac{u}{(1+u)^3}\left\langle \int_{2u/3\chi}^{\infty} K_{5/3}(x)\,dx + \frac{u^2}{1+u}K_{2/3}\left(\frac{2u}{3\chi}\right)\right\rangle; \tag{3.1}$$

Here we have introduced the following notation: $u = \omega/(E-\omega)$, $\chi = E|\nabla U|$ is the ratio of the energy of the particles to the critical energy $E_c^{(2)}$, the K_ν are Macdonald functions, and the angle brackets denote the averaging mentioned above. The second term in the brackets, which is proportional to u^2, is the result of the interaction of the spin of the electron with the photon being emitted. The classical results[4,89,90,94] are obtained from (3.1) in the limit of relatively low frequencies ($u \ll 1$). Just as in the classical lim-

it,[4,89] the averaging over time and the impact parameters for superbarrier particles in the row case can be reduced to a single integration over the permissible interval of distances to the crystallographic row (see also Ref. 6, p. 224).

According to (3.1), for low values of the parameter $\chi \ll 1$, the frequency ω at which the maximum of $dW/d\omega$ is reached increases in proportion to the square of the energy of the particle E^2, while the value of $dW/d\omega$ at the maximum does not depend on E. Here the total energy losses of the particle in emission are proportional to E^2.[90,96] At superhigh energies ($\chi \gtrsim 1$), the pattern substantially changes. In particular, at sufficiently high parameters $\chi \gg 1$, the frequency of the maximum is proportional to only the first power of the energy, instead of to E^2. At the same time, the value of $dW/d\omega$ at the maximum when $\chi \gg 1$ declines as $E^{-1/3}$. Consequently the total energy losses in emission are now equal to $E^{2/3}$ (see Sec. 3.2). Graphs of the spectrum of (3.1) for fixed values of χ, as well as graphs of the total energy losses, are given, e.g., in Ref. 97.

In analyzing the emission spectra of particles, channeled or superbarrier, but close in their transverse energy to the height of the potential barrier, one must also perform an averaging over the possible trajectories of the particles in the initial state, i.e., over the values of the parameter χ corresponding to these trajectories.

The region of highest intensity of the electric field of the planes or rows of the crystal corresponds to distances approximately equal to the amplitude of the thermal vibrations of the atoms. Although the dimensions of this region are small in comparison with the area per plane or row of the crystal, its contribution to the emission spectrum proves to be very substantial. As the ratio of the temperature of the crystal to the Debye temperature varies, the averaged potential, and particularly its gradient, vary most strongly precisely in the region of the radius of the thermal vibrations from the plane or row (see Table X). This leads to a relatively strong temperature dependence of the total energy losses[99] and of the emission spectra (3.1) of particles of superhigh energy.

The result of averaging the spectrum of (3.1) over all possible trajectories of electrons of energy $E = 150$ GeV incident at the angle $\theta_0 = 10^{-5}$ with respect to the $\langle 110 \rangle$ row of a germanium crystal at the temperature 100 K is shown by the solid curve in Fig. 18. This same diagram shows the results of the corresponding experiments[98] performed at CERN. Fig. 18a corresponds to electrons of energy $E = 150$ GeV, and Fig. 18b to positrons of the same energy; the solid dots correspond to zero angle of entry of the particles, the triangles to the angle $\theta_0 = 2.5 \times 10^{-5}$, and the open circles to the angle $\theta_0 = 9.6 \times 10^{-5}$.

First of all we note that, as the entry angle increases from zero to $\theta_L = 6.0 \times 10^{-5}$, the spectral energy density per unit path length for positrons increases, while conversely it falls for electrons. This is due to the differing behavior of the fraction of the particles that move most of the time in a region of relatively high field intensity. In the case of electrons the fraction of the particles with a transverse energy near the bottom of the potential well decreases rapidly with increasing entry angle from zero to θ_L. In the case of positrons the fraction of particles with transverse energy near the potential peak increases, conversely, as the angle increases from zero up to $\theta_L = (2U_0/E)^{1/2}$, where U_0 is the height of the peak. Thus the observed orientational dependence of the emission spectra within the limits indicated in Fig. 18 of the entry angles $0 < \theta_0 < 1.50\theta_L$ is due to the redistribution of the emitting particles over the distances to the closest row. As theoretical analysis[100] shows, at the target thickness of 185 μm used in the experiment, a particle moving in the region of maximum gradient of the potential could emit with appreciable probability several photons with some energy averaged over the spectrum. Since a detector with total absorption of the emitted energy was used to measure the photons, it is more correct to assume that the experimental points correspond to the emission spectrum weighted with the probability of emitting in the given target of differing numbers of photons. This implies a possible reason for the observed maximum in the spectrum at $\omega \approx 0.85\,E$, which is absent on the theoretical curve. Actually, if we take account of the multiplicity of emission of photons by an electron throughout the thickness of the target (as well as the background from incoherent bremsstrahlung due to the thermal vibrations of the lattice), as was done, e.g., in Ref. 146, then

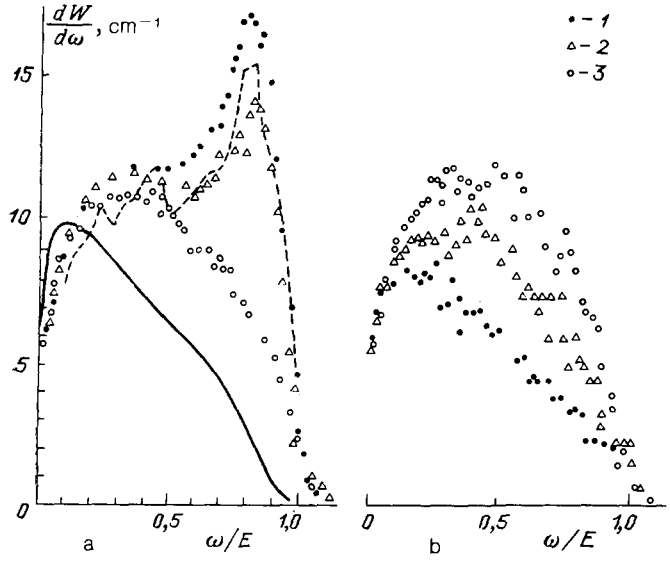

FIG. 18. Frequency dependence of the emission energy per unit path length in germanium at a temperature of 100 K as a function of the ratio of the photon energy ω to the initial energy of the particle $E = 150$ GeV. a–Case of electrons. b–Case of positrons. *1*–Zero entry angle θ_0 with respect to the $\langle 110 \rangle$ row, *2*–$\theta_0 = 2.5 \times 10^{-5}$, *3*–$\theta_0 = 9 \times 10^{-5}$. Solid curve–result of calculation for entry angle $\theta_0 = 10^{-5}$ without allowance for the multiplicity of the photons; dashed curve–calculation with this allowance.[146]

the results of calculation (dotted curve in Fig. 18a) become far closer to experiment (dots). Thus the appearance of the stated maximum is a consequence of the superposition in the detector of several softer photons. The superposition effect becomes more substantial with decreasing entry angle θ,[147] with increasing target thickness, and with increasing efficiency of the photon detector.

3.2. Radiative energy losses

At superhigh energies, the influence of emission on the process of channeling of particles in crystals increases. This problem was treated rather long ago theoretically,[80–82] but there the treatment was restricted to the case of relatively low energies at which the energy losses are due to emission of relatively soft photons ($\omega \ll E$). The parameter that determines the influence of emission is the variation of the transverse energy $d\varepsilon/dt$ per unit time owing to emission. In the classical approach one can calculate the work done by the radiative frictional forces and obtain the relation between the losses of transverse energy and the losses of total energy of channeled particles per unit time in the form[6,80]

$$\frac{d\varepsilon}{dt} = \frac{dE}{dt}\left(E^{-2} + \frac{v_\perp^2}{2}\right). \tag{3.2}$$

Here $v_\perp$ is the transverse component of the velocity of the particle with respect to the row or plane.

Here the losses of total energy are associated with the potential gradient by the relationship

$$\frac{dE}{dt} = -\frac{2e^2}{3}E^2(\nabla U)^2. \tag{3.3}$$

At superhigh energies $E \gg E_c^{(1)}$, the second term in the parentheses in (3.2) dominates, and hence we have

$$\frac{d\varepsilon}{dt} = \frac{v_\perp^2}{2}\frac{dE}{dt}. \tag{3.4}$$

Equation (3.4) remains in force also in the case in which the energy of the emitted photons ω is not necessarily small in comparison with the initial energy of the particle, while the emission process is substantially of quantum type.[106] At the same time, the classical expression (3.3) for the losses of total energy is not valid when the energy of the emitted photons is comparable with the energy of the particle. Actually, when $E \sim E_c^{(2)} \gg E_c^{(1)}$, the angle $v_\perp$ at which the particle moves with respect to the row or plane of the crystal considerably exceeds the effective angle of emission E^{-1} with respect to the direction of the instantaneous velocity. Therefore, in the emission process the transverse velocity $v_\perp$ (the angle of motion of the particle) practically does not change. The change in the potential energy of the particle in the emission process can also be neglected owing to the relative smallness of the coherent length of the emission. Consequently, in the emission of a photon of energy ω, the transverse energy of the particle changes by the amount:

$$\Delta\varepsilon = \frac{Ev_\perp^2}{2} - \frac{E-\omega}{2}v_\perp^2 = \frac{\omega}{2}v_\perp^2.$$

Here we have taken account of the fact that the kinetic energy of transverse motion is proportional to the relativistic mass of the particle. Since $\omega = \Delta E$, we arrive at Eq. (3.4), apart from the dependence on the magnitude of ω/E.

The losses of the total energy dE/dt in the general case are determined by the local value of the field intensity and the magnitude of the parameter χ (see (3.1)), while the losses of transverse energy are determined also by the magnitude of the transverse velocity of the particle. In particular, at high enough energies $E \gg E_c^{(2)}$, when $\chi \gg 1$, we obtain instead of the classical expression (3.3) for the energy losses E per unit time the following (see, e.g., Ref. 97):

$$\frac{dE}{dt} \approx -0{,}82e^2\chi^{2/3}.$$

The emission process leads on the average to a decrease in the transverse energy, in contrast to the incoherent scattering of particles by the electrons and atoms of the lattice (see Sec. 2). The presented results imply that, in the emission of a hard enough photon ($u \gtrsim 1$), the particle can lose the greater part of its transverse energy. As was noted above, one must take account of this effect in the kinetic equations that describe the dynamics of motion of light channeled particles, such as electrons and positrons, at superhigh energies.

We note that 17% losses of the total energy of the electrons in a germanium target 185-μm thick were observed in the experiment of Ref. 98. Since the radiation length of germanium is 2.3 cm, the energy losses per unit length in this case exceeded the losses in an amorphous medium by a factor of about 20.

3.3. Formation of electron-positron pairs at relatively small entry angles of photons

The process of pair formation by a photon in a crystal is closely connected with the process of emission of a photon by a charged particle, owing to the cross-symmetry of the amplitudes of reaction. If in the amplitude of emission by an electron we perform the substitution $\omega \to -\omega$, interpret an electron in the initial state with energy E as giving rise to a positron with energy $-E$, and also take account of the change in density of the number of final states for the two processes being studied, then we can easily derive from the expression for the emission probability a corresponding expression for the probability of pair formation by a photon. Here the parameter $u = \omega/(E-\omega)$ (see 3.1) in the case of pair formation goes over into $-\tilde{u}$, where $\tilde{u} = \omega(\omega - E)^{-1}$. The parameter $\tilde{u}$ is always greater than unity; therefore the process of pair formation is associated with the emission process of sufficiently hard photons, for which correspondingly we have $u > 1$.

Since, as was noted above, a threshold energy exists for a channeled electron for emitting hard photons ($u > 1$), a threshold energy also exists of a photon $\omega_c = 2/U_0$, entering parallel to a row or plane below which pair formation in the averaged potential of the planes or rows of depth U_0 is impossible. The existence of a threshold ω_c, as in the case of emission of hard photons, is a consequence of the laws of conservation of energy and longitudinal momentum of the particles. As was shown in Refs. 94 and 96, one can find the quantity ω_c also from the condition of equality of the angle of separation of the pair $\sim 1/\omega$ to the critical angle of channeling for the particles being created $\theta_L = (2U_0/E)^{1/2}$ (where $E \approx \omega/2$).

Within the constant-field approximation (CFA) for photon energies ω that substantially exceed the threshold energy ω_c, the probability of pair creation per unit time differentiated with respect to the energy E of the created posi-

tion is obtained by cross-transformation from (3.1) and has the form

$$\frac{dw^{(p)}}{dE}=\frac{e^2}{\pi\sqrt{3}\omega^2}\left\langle\frac{\tilde{u}^2}{\tilde{u}-1}K_{2/3}\left(\frac{2\tilde{u}}{3\chi}\right)-\int\limits_{2\tilde{u}/3\chi}^{\infty}K_{5/3}(x)\,dx\right\rangle. \tag{3.5}$$

The brackets in this case denote averaging over all transverse coordinates of the point of pair formation. The total probability of formation of an electron-positron pair in a germanium crystal 1.4-mm thick at the temperature 100 K, when the photons entered parallel to the ⟨110⟩ row, was measured at CERN[101] as a function of the photon energy. The results are represented by dots in Fig. 19. The solid curve represents the results of calculation by (3.5), to which is added a component of the probability involving pair formation due to thermal fluctuations of the averaged potential of the row. It was assumed that this component of the probability practically does not differ from the corresponding probability for the case of an amorphous medium and corresponds to a plateau at the level of unity on the ordinate row. The calculations agree within the limits of experimental error with the measurements performed at zero entry angle for all photon energies > 22 GeV, which prove to be rather far from the threshold $\omega_c \approx 1.9$ GeV.

Since the crystal does not influence the motion of the photons up to the instant of pair formation, the distribution over the transverse coordinates of the points of pair formation does not depend on the entry angle of the photon with respect to the row or plane, and the averaging in (3.5) cannot lead to an orientational dependence of the probability of pair formation, in contrast to the case of emission in (3.1). On the other hand, the experiments of Ref. 101 revealed an orientational dependence of the probability of pair formation over a rather broad variation of entry angles of the photons as compared with the Lindhard angle (several milliradians). This indicates the limitation of the theory, which is based on the constant-field approximation, in particular, at relatively large ($\theta_0 \gg \theta_L$) entry angles of the particles. On the other hand, the experiments on emission and pair formation in crystals performed as early as the 60s at relatively large entry angles agreed well with the theory of coherent bremsstrahlung and pair formation based on the Born approximation.[102] There is a close connection between these two mechanisms of emission and pair formation, which we shall discuss below.

3.4. Limits of applicability of the constant-field approximation and coherent effects

As we have already mentioned, the constant-field approximation (CFA) of (3.1) and (3.5) is applicable if the maximum angle of deflection of the charged particles by the field of the planes or rows considerably exceeds the effective angle of emission ($\sim 1/E$) or the angle of separation of the pair ($\sim 1/\omega$). When the particles enter at an angle $\theta_0 \lesssim \theta_L$, where $\theta_L = (2U_0/E)^{1/2}$ is the Lindhard channeling angle, the angles of deflection of charged particles θ_d while moving in the crystal are of the order of the quantity θ_L. Therefore, at such entry angles the condition of applicability of the CFA is satisfied at energies sufficiently large in comparison with $E_c^{(1)} = 1/U_0$. However, with increase in the entry angle, the angles of deflection of the particles by the field decrease, and the CFA ultimately loses force, even at superhigh energies $E \gg E_c^{(1)}$.

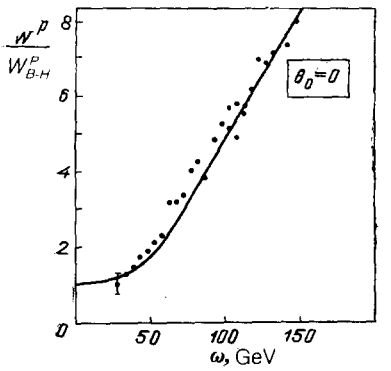

FIG. 19. Total probability of formation of an electron-positron pair by a photon incident along the ⟨110⟩ row of germanium at a temperature of 100 K as a function of the energy of the photon. The corresponding probability for an amorphous target $w^{(p)}_{B-H}$ does not depend on the energy and is taken to be unity.

Let the entry angle θ_0 substantially exceed the Lindhard angle θ_L. Then the angle of deflection θ_d of the particles by the field is determined by the equation (see, e.g., Ref. 96) $\theta_d \approx U_0/E\theta_0$, while the condition of applicability of the CFA imposes the following restriction on the entry angles: $\theta_0 \ll U_0$. Interestingly, the angle $\theta_c \equiv U_0$ at which the CFA loses force does not depend on the energy of the particles. However, since it is assumed that $\theta_c \gg \theta_L$, we are dealing with relatively high energies $E \gg E_c^{(1)}$. The values of the entry angle $\theta_c \equiv U_0$ at which the CFA breaks down are given in Table X.

In the opposite limit $\theta_0 \gg \theta_c$ the deflection angles of the particle by the field are small in comparison with the effective emission angles $1/E$. Hence the emission is of dipole character (see, e.g., Ref. 95). In this case the formation length of the emission (coherent length) $l_{coh} \approx u/E$ becomes comparable in order of magnitude with the distance through which the particles pass between two successive collisions with rows or planes. As a result, the processes of emission and pair formation generally occur coherently at a large enough number of rows or planes, in contrast to the case in which the CFA holds. Thus, in the limit of relatively large entry angles $\theta_0 \gg \theta_c$, the probabilities of the processes being discussed in the averaged potential of the rows or planes coincide with the corresponding probabilities calculated within the framework of the standard theory of coherent bremsstrahlung and pair formation,[102,103] which is based on the Born approximation for the interaction of the particles with the atoms of the crystal. According to the standard theory, the derivative of the probability of pair formation with respect to the positron energy per unit time by a photon entering at a relatively large angle $\theta_0 \gg \max\{\theta_L, \theta_c\}$ to the crystallographic row can be represented in the form (see, e.g., Ref. 4)

$$\frac{dw^{(p)}}{dE}=\frac{e^2}{\omega^2}\sum_{\mathbf{g}}\frac{g^2}{gv}|U(\mathbf{g})|^2\left[1-\frac{\tilde{u}^2}{2(\tilde{u}-1)}-2\Omega_n+2\Omega_n^2\right]\eta(1-\Omega_n); \tag{3.6}$$

Here ν is a unit vector in the direction of entry of the photon, the $\mathbf{g}$ are reciprocal-lattice vectors orthogonal to the crystallographic row, $\Omega_n = \tilde{u}/2E\mathbf{g}\nu$.

$$U(\mathbf{g}) = \frac{1}{S}\int_S U(\boldsymbol{\rho})\, e^{-i\mathbf{g}\boldsymbol{\rho}}\, d^2\rho \tag{3.7}$$

is the Fourier transform of the averaged potential $U(\boldsymbol{\rho})$ of the row. The integration in (3.7) is performed over the area S of the unit cell in the plane orthogonal to the row. The Fourier transform (3.7) in the case of a monatomic crystal involves the three-dimensional Fourier transform of the atomic potential $\varphi(\mathbf{k})$ by the relationship $U(\mathbf{g}) = V^{-1}\exp(-g^2u_T^2)\varphi(g_x,g_y,0)$, where V is the volume of the unit cell of the crystal, and u_T is the amplitude of the thermal vibrations.

If at entry angles $\theta_0 \gg \max\{\theta_L, \theta_c\}$ the azimuthal direction φ of entry of the particles with respect to the chosen crystallographic row is far from the directions of the planes having rather low Miller indices, then a large number of two-dimensional vectors $\mathbf{g}$ contribute to the probability of the process, and we can replace the summation in (3.6) with integration over $(2\pi)^{-2}Sd^2g$. Thus the interference from different rows proves to be inessential. The interference from different rows is inessential apart from a dependence on φ in the case in which the entry angle θ_0 is close to the Lindhard angle θ_L. Here, as was noted in Sec. 2.a, the trajectories of the particles undergo a strong bending in the plane orthogonal to the rows. Consequently the collisions with the different rows are uncorrelated in time, even if the initial direction of entry coincides with the direction of one of the low-index planes. However, at energies $E \gg E_c^{(1)}$, the angle θ_c exceeds θ_L. Hence, as the entry angle θ_0 is decreased, the standard theory of emission based on the Born approximation (3.6) breaks down earlier (at $\theta_0 \sim \theta_c$) than the effects of channeling become substantial.

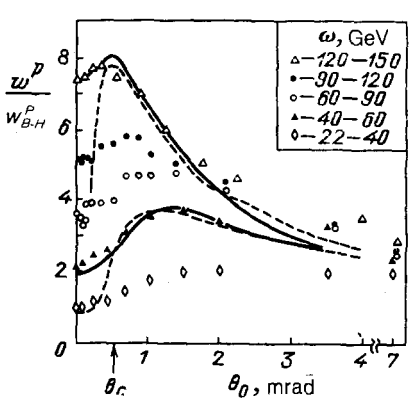

FIG. 20. Probability of pair formation by a photon in a germanium crystal, divided by the corresponding probability for an amorphous target, as a function of the entry angle θ_0 of photons with respect to the ⟨110⟩ row for different intervals of photon energies. The dashed curves show the results of calculations according to the theory of coherent pair formation based on the Born approximation with account taken of the incoherent background; the solid curves correspond to calculations based on the more rigorous theory taking account of the influence of the bending of the trajectories of the charged particles by the averaged potential of the row on the probability of pair formation. The upper curves correspond to the open triangles, and the lower curves to the solid triangles. The arrow on the angle axis shows the theoretical value of θ_c at which the Born approximation should break down.

Figure 20 shows the results of measuring[101] the probability of pair formation in a germanium crystal 1.4-mm thick at a temperature of 100 K as a function of the entry angle of the photons with respect to the ⟨110⟩ row. The azimuthal direction of entry was chosen such that the beam of photons made an angle of 0.1 radians with the (001) plane. The experimental results correspond to the different intervals of energies of the incident photons indicated in the diagram. The dotted curves show the corresponding calculations by the theory of coherent pair formation of (3.6) with the addition of an incoherent background involving the thermal vibrations of the atoms. As we see from the presented results, the theory of coherent pair formation agrees rather well with the measurements when the entry angle exceeds about 5×10^{-4} radians. However, at smaller angles one observes an appreciable deviation from the predictions of the standard coherent theory. If now we turn to Table X, we easily see that $\theta_c = 5.3\times10^{-4}$ is precisely the angle, according to the presented ideas, that separates the region of applicability of the CFA and the coherent theory. We note for comparison that the Lindhard angle $\theta_L = 2U_0^{1/2}\cdot\omega^{-1/2}$ in the case being discussed amounts to 8.5×10^{-5} at $\omega = 150$ GeV and 2.2×10^{-4} at $\omega = 22$ Gev, which is severalfold smaller than the angle θ_c.

Thus the influence of channeling, or more exactly, the influence of bending of the trajectories, has the result that, at zero angles of entry of the photon, the total probability of pair formation does not approach zero, as is predicted by the standard theory based on the Born approximation, but reaches a value that can considerably exceed the incoherent background. As we see from Fig. 19, this value agrees well with calculations based on the CFA.

Strictly speaking, for superhigh energies $E \gg E_c^{(1)}$ the coherent theory is applicable only for entry angles $\theta_0 \gg \theta_c$, and the CFA for angles $\theta_0 \ll \theta_c$. As regards the neighborhood of entry angles θ_0 close in order of magnitude to θ_c, here we need a theory devoid of restrictions on the ratio of the angle of deflection of the particle by the field to the effective emission angle. Such a theory has been developed in a number of studies for the planar[88,106,108] and row[96,101,104,105,109] cases.

3.5. The theory of emission and pair formation for $\theta_0 \gtrsim \theta_L$

There are several approaches for solving the problem of emission and electron-positron pair formation in the case in which the constant-field approximation or the standard theory of coherent electromagnetic processes in crystals based on the Born approximation is inapplicable.

The first approach is based on formulas derived by an operator quasiclassical method for the probabilities of the processes being studied in rather arbitrary external fields.[97,135,136] Here, the quantum character of the motion of the high-energy particles in the external field is neglected from the outset, but the quantum character of the emission of a photon is taken into account. As a result one can express the probability of emitting a relatively hard ($u \sim 1$) photon and the probability of pair formation in the form of functionals that depend on the classical trajectory of the charged particles. In the case in which the particles move in the crys-

tal near principal directions, the external field is considered to be the field of the atoms of the crystal averaged along the rows or planes.

This approach leads most rapidly to the required results. However, owing to the assumptions adopted at the outset, it requires additional justification and estimates of the accuracy of the obtained expressions (see, e.g., Refs. 137 and 138).

In another approach one uses as the starting point the results of the quantum theory of emission and pair formation in the averaged potential of the rows or planes.[6,82,88] Under conditions of channeling or superbarrier motion, one can to a certain degree separate the longitudinal and transverse motion of the particles; in the starting formulas the probabilities of the processes being discussed are expressed in terms of the matrix elements of the radiative transitions between the states of the transverse motion. At high enough energies the number of states of the transverse motion is large, while the transverse wave functions can be taken in quasiclassical form. As a result, as was shown in Ref. 106, under certain extra conditions the probabilities actually can be expressed in the form of functionals of the classical trajectory of the transverse motion. In this approach the conditions of applicability of the expressions that are obtained become more concrete. In particular, under the condition that the square of the entry angle θ_0^2 substantially exceeds the square of the Lindhard angle $\theta_L^2 = 2U_0/E$, and under the condition that we can neglect the interference from neighboring rows, the spectral-angular density of the probability of pair formation by a photon per unit path in the crystal can be represented in the form

$$\frac{d^2w^{(p)}}{dE\,do} = \frac{e^2}{2\pi^2}\frac{E^2}{\omega}\frac{\theta_0}{S}\int_0^\infty \left[\left(1-\tilde{u}+\frac{\tilde{u}^2}{2}\right)|\mathbf{J}_\rho - J_z\mathbf{n}_\rho|^2 + \frac{\tilde{u}^2}{2E^2}|J_z|^2\right]dx, \tag{3.8}$$

$$J_z = \int_{-\infty}^{\infty} e^{-ig(\rho)}dy,\quad \mathbf{J}_\rho = \int_{-\infty}^{\infty}\boldsymbol{\theta}_d(\rho)\,e^{-ig(\rho)}dy,$$
$$g(\rho) = \frac{\omega(\tilde{u}-1)}{2\theta_0}\int_0^y (|\boldsymbol{\theta}_d(\rho)-\mathbf{n}_\rho|^2 + E^{-2})\,dy. \tag{3.9}$$

Here the angle $\boldsymbol{\theta}_d$ of deflection of an electron (or positron) of energy E on the trajectory by the field of a row is determined by the equations

$$\theta_d^{(x)}(\rho) = -\frac{1}{E\theta_0}\int_{-\infty}^{y}\frac{\partial U}{\partial x}dy,\quad \theta_d^{(y)} = -\frac{1}{E\theta_0}U(\rho);$$

$U(\rho)$ is the potential of the row, ρ is the distance to the row, $\mathbf{n}_\rho = \{\theta\cos\varphi,\ \theta\sin\varphi\}$; θ and φ are the polar and azimuthal angles of exit of the charged particle, $do \approx \theta\ d\theta\ d\varphi$, the yz plane is formed by the crystallographic row and the direction of entry of the photon of energy ω. For relatively large entry angles $\theta_0 \gg U_0$, the dipole approximation is valid. Within its framework we have

$$\mathbf{J}_\rho \approx \int_{-\infty}^{\infty}\boldsymbol{\theta}_d(\rho)\exp\left[-\frac{i\omega(\tilde{u}-1)}{2\theta_0}(\theta^2+E^{-2})\,y\right]dy,$$
$$J_z \approx 2\mathbf{n}_\rho\mathbf{J}_\rho(\theta^2+E^{-2})^{-1}.$$

This corresponds to the results of the theory based on the Born approximation. In the opposite limit $\theta_L \lesssim \theta_0 \ll U_0$, in calculating the integrals $\mathbf{J}_\rho$ and J_z one can apply the stationary-phase method, which leads to the results of the CFA of (3.5).

In the planar case, in contrast to the row case, the periodicity of the collisions with planes is always essential for superbarrier particles, and the corresponding result for the differential probability of pair formation has the form

$$\frac{d^2w^{(p)}}{dE\,do} = \frac{e^2E^2}{2\pi\omega}\sum_{n=1}^{\infty}\left\{\left(1-\tilde{u}+\frac{\tilde{u}^2}{2}\right)|J_n^{(x)}-\alpha J_n^{(z)}|^2 + \left[(1-\tilde{u})\beta^2+\frac{\tilde{u}^2}{2}(\beta^2+E^{-2})\right]|J_n^{(z)}|^2\right\} \times\delta\left[\frac{\tilde{\omega}}{2}(\theta^2+E^{-2}+\langle\theta_d^2\rangle)-\omega_n\right]; \tag{3.10}$$

Here we have $\alpha = \theta\cos\varphi$, $\beta = \theta\sin\varphi$, $\tilde{\omega}_n = 2\pi n\theta_0/d$, $\tilde{\omega} = \omega(\tilde{u}-1)$, d is the interplanar spacing, δ is the Dirac function, and we have

$$J_n^{(x)} = T^{-1}\int_0^T \theta_d(t)\,e^{-if(t)}dt,$$

$$J_n^{(z)} = T^{-1}\int_0^T e^{-if(t)}dt,$$

$$f(t) = \tilde{\omega}\left[-\alpha\int_0^t\theta_d(\tau)\,d\tau + \frac{1}{2}\int_0^t(\theta_d^2(\tau)-\langle\theta_d^2\rangle)\,d\tau\right]-\omega_n t. \tag{3.11}$$

The angle of deflection θ_d and its mean-square $\langle\theta_d^2\rangle$ over the period are expressed in terms of the interplanar potential $U(x)$ in the form

$$\theta_d(t) = (E\theta_0)^{-1}(\langle U\rangle - U(x)),\quad x = t\theta_0,$$
$$\langle\theta_d^2\rangle = (E\theta_0)^{-2}(\langle U^2\rangle - \langle U\rangle^2).$$

Here the averaging on the right-hand side is performed over the transverse coordinate x within the limits of the interplanar interval d.

Concrete calculations using (3.8) and (3.10) have been performed[106] for model potentials $U(\rho)$ of an axis and $U(x)$ of planes of rather simple form. Thus, for the model of a row potential $U(\rho) = U_0 a/\rho$, where U_0 and a are constants that depend on the type of crystal and Miller indices, the quantities J_z and $\mathbf{J}_\rho$ are expressed in analytic form, which substantially simplifies the subsequent numerical calculations.

For the planar potential $U(x) = -U_0(2x/d)^2$, where $|x| < d/2$, the quantities entering into (3.10) can be represented in the form

$$J_n^{(z)} = \int_0^1 \cos f(\eta)\, d\eta, \quad J_n^{(x)} = -\frac{p}{E}\int_0^1 (1-3\eta^2)\cos f(\eta)\, d\eta,$$

$$f(\eta) = \frac{3}{2}\tilde{u}\alpha E_c^{(2)} p^2 (\eta - \eta^3)$$

$$+ \frac{27\tilde{u}E_c^{(2)}}{4E} p^3 \left(\frac{\eta}{45} - \frac{2}{9}\eta^3 + \frac{1}{5}\eta^5\right) + \pi n \eta,$$

$$\langle \theta_d^2 \rangle = \frac{4p^2}{5E^2}. \tag{3.12}$$

Here we have $p \equiv U_0/3\theta_0$, $E_c^{(2)} = d/U_0$, and E is the energy of the positron that is formed.

The total probability of pair formation per unit path as a function of the entry angle of the photon θ_0 with respect to the planes in the case of arbitrary p can be obtained only by numerical integration of (3.10) with respect to the azimuthal angle φ and the positron energy E. For relatively small entry angles, when $p \gg 1$, the total probability is expressed in analytic form

$$w^{(p)} = \frac{4e^2\omega}{\pi^2}\left(\frac{U_0}{d}\right)^2 \sum_{n=1}^{\infty}\left(\frac{\xi_n}{n}\right)^2 \left[\left(1 + \xi_n - \frac{\xi_n^2}{2}\right)\right.$$

$$\times \ln\left\{\frac{2}{\xi_n}[1 + (1-\xi_n)^{1/2}] - 1\right\}$$

$$\left. - (1+\xi_n)(1-\xi_n)^{1/2}\right] \eta(1-\xi_n), \tag{3.13}$$

where $\xi_n = d/(\pi n \omega \theta_0)$, and η is Heaviside's step function. In the opposite limit $p \ll 1$, the corresponding result also has the rather simple form

$$w^{(p)} = \frac{4e^2\omega}{\pi^2}\left(\frac{U_0}{d}\right)^2 F(\zeta),$$

$$F(\zeta) = 4\cdot 3^{3/2}\pi\zeta^2 \int_0^1 \frac{y}{1-y^2}\left[\zeta\left(\frac{2y}{1-y^2} - \ln\frac{1+y}{1-y}\right) K_{1/3}\left(\frac{4\zeta}{1-y^2}\right)\right.$$

$$\left. + yK_{2/3}\left(\frac{4\zeta}{1-y^2}\right)\right] dy,$$

$$\zeta \equiv \frac{d}{6U_0\omega}. \tag{3.14}$$

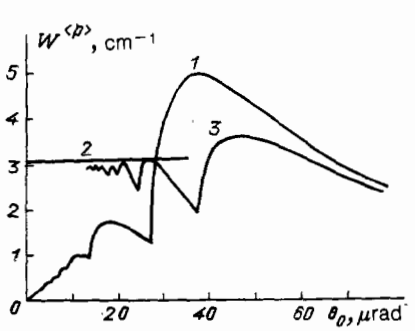

FIG. 21. Probability of creation of an electron-positron pair by a photon of energy $\omega = 3$ TeV per unit path length in a germanium crystal as a function of the entry angle with respect to the (110) plane. Curve *1*–Born approximation of (3.13), *2*–constant-field approximation of (3.14), *3*–theory taking account of the non-dipole character of the process at high energies. $U_0 = 39$ eV, $d = 2.0$ Å.

The orientational dependence (Fig. 21) in the planar case as calculated by using (3.11) and (3.12) is fully analogous to that which was calculated in Ref. 101 for an isolated row on the basis of the quasiclassical approach and the model of the row potential $U(\rho) \sim 1/\rho$ (Ref. 105) (solid curves in Fig. 20). In the row case, as was mentioned above, the effects of non-dipole character of the emission and the associated deviations from the standard theory set in earlier, even at energies of several tens of GeV. It has been proposed to perform in the future[100] experiments in the region of even higher energies $E \sim 1$ TeV, at which the discussed effects can be manifested also in the planar case.

4. POSSIBILITIES FOR CHANNELING OF NEUTRAL PARTICLES

4.1. Requirements on the periodic structures

The advances in employing channeling phenomena of charged particles in crystals to control beams of particles have stimulated the search for possibilities for channeling neutral particles, in particular, photons of the x-ray and γ range, as well as thermal and resonance neutrons.[110–118] In the case of photons whose energy considerably exceeds the binding energy of the K electrons of the atoms of the material, the real component of the dielectric susceptibility $\chi'(\omega)$ has the form

$$\chi'(\omega) = -\frac{\omega_p^2}{\omega^2}. \tag{4.1}$$

Here $\omega_p = (4\pi n e^2/m)^{1/2}$ is the plasma frequency of the electrons of the material, n is their number density, and m is the mass of an electron. Since for most materials we have $\omega_p \sim 10$ eV, the susceptibility in the x-ray range is small and negative. This means that, at the phase boundary of two materials, x-ray photons can be totally reflected from the material having the higher value of $|\chi'|$, while the angle of incidence of the photons with respect to the boundary must not exceed $\theta_c = |\Delta\chi'|^{1/2}$, where $\Delta\chi'$ is the jump in the dielectric susceptibility.

Neutrons interact mainly with the nuclei of materials. The real component of the nuclear susceptibility $\chi'(\lambda)$ is associated with the amplitude a of coherent scattering of neutrons by the nucleus averaged over the isotopes, and with the number density of the nuclei of the substance N by the relationship

$$\chi'(\lambda) = -\frac{\lambda^2 a N}{\pi}. \tag{4.2}$$

Here $\lambda = 0.287E^{-1/2}$ is the neutron wavelength in Å, and E is its kinetic energy in eV. If the energy of the neutron is far from the energy of resonance in scattering, then the scattering amplitude $a \sim 3\cdot 10^{-13}$–10^{-12} cm is positive for most substances, although there are exceptions, e.g., Ti, Mn, and Li, for which $a < 0$. Thus the critical angle for total reflection $\theta_c = |\Delta\chi'|^{1/2}$ for thermal neutrons ($E \sim 10^{-2}$ eV) proves to be approximately as small ($\sim 10^{-3}$) as for photons in the x-ray range ($\omega \sim 10$ keV). We should note that the phenomenon of small-angle reflection of x-ray photons and thermal neutrons has been employed for a long time in the elements of x-ray optics,[125] and also for transport[119–123] and rotation[124,126] of beams of particles with cylindrical tubes.

In principle in ordinary crystals a modulation exists of the electron and nuclear density with a period of the order of

the lattice constant. At first glance a phenomenon should exist of total reflection of x-ray photons and neutrons incident at sufficiently small angles to the crystallographic planes or axes. However, there is a substantial difference in the characters of the interaction of charged and neutral particles with a crystal. As was shown in Refs. 110–117, it leads to the impossibility of channeling of neutral particles in ordinary crystals.

The requirements on the parameters of the structure necessary for the existence of a channeling effect can be obtained from the following simple considerations.[114,115] Let a particle be incident at the critical angle θ_c to the planes of the crystal. The characteristic parameter that determines the degree of localization of the particle in the direction orthogonal to the planes is the quantity $\lambda_\perp = \lambda/\theta_c$, where λ is the de Broglie wavelength of the particle. For x-ray photons with energy ω we obtain: $\theta_c = \omega_p/\omega$, where ω_p is a certain average over the volume of the value of the plasma frequency of the electrons of the crystal. Hence we have $\lambda_\perp \approx 2\pi/\omega_p$. We note that, for the energy region of photons in which Eq. (4.1) holds for the dielectric constant, the magnitude of $\lambda_\perp$ does not depend on the energy of the photon and amounts to from 155 Å for gold to 377 Å for aluminum. This exceeds by two orders of magnitude the maximum interplanar spacings in crystals. Thus an x-ray photon in a crystal cannot be localized within a single channel. An analogous pattern exists also in the case of neutrons, whose transverse wavelength $\lambda_\perp = (4\pi N|a|)^{1/2}$ also amounts to a quantity of the order of 100 Å. However, the necessary conditions for channeling of neutral particles exist in structures formed by layerwise sputtering or deposition of different materials,[110–114] in bulk superlattices made of vacuum (or gas) cavities in metals, and other composites.[115–117]

4.2. Channeling in superlattices

The technology of preparation of layered structures with periods up to several tens of Ångström units by successive deposition of two different materials on a substrate has currently reached a very high level. Thus one obtains layers of rather large area ($\sim 10\ \text{cm}^2$) with a thickness error at the level of a monatomic layer. Periodic structures having a number of layers of several tens are used, in particular, at present for diffraction of soft x-rays with wavelengths ~ 10 Å,[128] as well as diffraction of cold neutrons ($E \approx 10^{-4}$–10 eV).[129] One can also obtain by an analogous method layered structures with a greater period $\sim 10^3$ Å suitable for observing the effect of channeling of photons and neutrons. However, we should note that for channeling purposes one need not at all maintain periodicity of the layers, in contrast to diffraction problems, where strict periodicity is an indispensable condition for coherence of scattering from many tens of planes. On the other hand, channeling requires a far greater number of layers, since the particles must enter through the end surface, whose area must be comparable with the cross section of the particle beam.

Let the electromagnetic wave enter at a sufficiently small angle $\theta \ll 1$ to the planes of the layered medium. The dependence of the electric field E of the wave of frequency ω on the longitudinal coordinate z is determined in this case by the coefficient $\exp(ik_z z)$ with a constant value of the longitudinal component of the wave vector k_z, while the dependence on the transverse coordinate x is determined by the equation[127]

$$\frac{\partial^2 E}{\partial x^2} + \left[\frac{\omega^2}{c^2}(1 + \chi(\omega, x)) - k_z^2\right] E = 0. \tag{4.3}$$

In deriving (4.3) it was assumed that the wave is polarized perpendicular to the plane of incidence. However, at small angles of incidence θ the polarization proves to be inessential, and the same equation holds for the case of parallel polarization of the incident radiation.[125] The dependence of the dielectric susceptibility $\chi(\omega, x)$ on the coordinate x is determined by the profile of the deposited layers. In the simplest case it can be given in the form of a rectangular comb function.[110] The quantity $k_x^2 = \omega^2 c^{-2} - k_z^2$ in Eq. (4.2) has the meaning of the mean square of the transverse momentum of the photon for the different states of the field in the medium.

The amplitudes of the field in the different states are determined by the coefficients of the expansion of the plane wave corresponding to the particles entering the layered medium in the eigenfunctions of Eq. (4.3). Localized states can be effectively excited at entry angles smaller than the critical angle $\theta_c = |\Delta\chi|^{1/2}$, where $\Delta\chi$ is the jump in dielectric susceptibility at the boundary of the layers. The passage of particles through a layered structure in such states must be accompanied by a decrease in their absorption in comparison with the mean absorption that occurs at relatively large entry angles $\theta \gg \theta_c$. In the exit of the beam of neutral particles from the medium, just as in the case of electrons of MeV energies,[5] one should also observe a characteristic angular dependence with maxima corresponding to the allowed value of the transverse momentum k_x in the medium.

An interesting phenomenon exists in the physics of radiation damage, in which vacuum or gas cavities appear in crystals under the action of an intense flux of ions, neutrons, or electrons. Under certain conditions such cavities can form ordered structures, or superlattices. As a rule the symmetry of the superlattices coincides with the symmetry of the crystal, and here the cavities have a spherical form, practically identical radii, which varies from lattice to lattice (20–100 Å), while the period of the superlattices amounts respectively to 200–1500 Å. Superlattices of cavities have been obtained in a set of metals and their alloys, preferentially with the bcc or fcc structures,[130] upon neutron or ion irradiation at high target temperatures. In crystals of CaF_2 and SrF_2 under the action of electrons in a transmission microscope with the target at room temperature,[131] formation of lattices made of spheres of Ca or Sr was observed. Under normal conditions the superlattices of cavities become highly stable structures.

Since the period of modulation of the electron and nuclear density in such structures considerably exceeds the corresponding period of the crystals, particles with relatively long (> 10 Å) wavelengths of the order of the superlattice constant can be diffracted in them, just as in the corresponding layered structures.[116,117,131] As regards particles with shorter wavelengths, as the wavelength and the entry angle decrease, diffraction is replaced by the effect of channeling.[115–117] Actually the Bragg angle is determined by the equation $\sin\theta_B = Hc/2\omega$, where $H \sim 2\pi/d$ is the modulus of the reciprocal-lattice vector (d is the interplanar spacing,

and c is the velocity of light). Within the framework of the two-wave theory of dynamical diffraction,[132] the angular width of the radiation being diffracted is determined by the equation $\Delta\theta \approx \chi'_H/\sin 2\theta_B$, where χ'_H is the corresponding Fourier transform of the susceptibility. With increasing frequency the Bragg angle declines, while the angular width $\Delta\theta$ increases. For small $\theta_B \ll 1$, the ratio $\Delta\theta/\theta_B$ has the form

$$\frac{\Delta\theta}{\theta_B} \approx 2\omega^2 |\chi'_H| (cH)^{-2}.$$

Since in the x-ray frequency region we have $\chi'_H \sim \omega_p^2/\omega^2$, we arrive at the conclusion[116,117] that, for lattices with interplanar spacing $d \gtrsim d_c = \lambda_p$, the width of the diffraction angle becomes comparable with the angle itself, which here is close in order of magnitude to the angle of "total Fresnel reflection" $\theta_c \approx \omega_p/\omega$. This means that the effective reflection of the photons occurs actually at a single lattice plane. That is, we arrive in this case at the possibility of channeling.

Under channeling conditions, in the expansion of the field of the incident wave in plane waves in the crystal, the main contribution comes from a relatively large number of reciprocal-lattice vectors orthogonal to a certain family of crystallographic rows (row channeling) or planes (planar channeling). This allows one in treating channeling in superlattices to restrict the treatment to the complex dielectric susceptibility $\chi = \chi' + i\chi''$ blurred along the rows or over the planes of the lattice, which in the case of charged particles corresponds to averaging the potential of the atoms of the lattice.

The number of localized states, which in the planar case is determined by (5.3), is small in the existing superlattices of cavities having constants $L \leqslant 1500$ Å. In this sense the channeling of neutral particles in them is analogous to the channeling of electrons of energies $E \lesssim 10$ MeV in crystals. In order to observe individual states of neutral particles in superlattices, the absorption must be low enough:[116] $n\chi''/\chi' \ll 1$ (n is the number of states). This condition can be satisfied for photons of energies ~ 100 keV and for thermal neutrons. With increasing superlattice constant, $L \gg \lambda_p$, the number of states increases, and ultimately one can assume that photons and neutrons are propagated along definite trajectories. In the planar case the trajectories of the particles are determined by the equation

$$z(x) = \int_{x_0}^{x} (\theta_0^2 + \chi'(\omega, x) - \chi'(\omega, x_0))^{-1/2} dx. \qquad (4.4)$$

Here z is the longitudinal coordinate; θ_0 and x_0 are respectively the angle and the point of entry of the particle with respect to the plane, $\chi'(\omega, x)$ is the susceptibility averaged over the plane. In the case of a plane of spherical cavities, for which $\chi(\omega,x) \sim x^2$, the trajectories of the channeled particles amount to a sinusoid having the period $T = (2\pi\omega/\omega_p)(S/\pi)^{1/2}$. The critical entry angle for channeling is determined by the depth of modulation of the susceptibility and has the form $\theta_c = (\omega_p/\omega)(\pi r_0^2/S)^{1/2}$, where r_0 is the radius of the cavities, and S is the area per cavity on the plane.

In addition to lattices made of vacuum or gas cavities, there are also other three- or two-dimensional structures (colloidal crystals)[107] with a suitable transition of modulation of the electron density, where it is also possible to observe channeling of photons and neutrons. In particular, certain forms of opal ($SiO_2 \cdot nH_2O$) consist of densely packed spheres of SiO_2 of diameter 10^3 Å, which form a rather perfect superlattice.[133,134]

To test the possibilities of channeling of x-ray photons an experiment was performed[139] in which the photons entered at a small angle to the plane formed by the rows of cylindrical microchannels in a glass matrix. The periodic structure amounted to a two-dimensional close-packed lattice of these cylinders with a period $d \approx 13$ μm and radius of cylinders $r = 5$ μm.

The dielectric susceptibility averaged over the plane depends on the distance x to the center of the plane channel according to the relationship

$$\chi(\omega, x) = \chi_0(\omega)\left\{1 - \frac{2r}{d}\left[1 - \left(\frac{x}{r}\right)^2\right]^{1/2}\right\}. \qquad (4.5)$$

Here $\chi_0(\omega)$ is the dielectric susceptibility of the continuous medium (glass). The trajectories of the photons entering at the angle θ_0 to the planes of the lattice are determined by Eq. (4.4). When $\theta_0 \ll (\chi'(\omega,0) - \chi'(\omega,r))^{1/2}$, most of the particles are captured into a channeling regime. The experiment was performed with a photon beam of energy $\hbar\omega = 22$ keV and an angular divergence at the entrance of $\Delta\Theta_0 \approx 0.2°$. A feature of photons of not too high energy is a substantial influence of absorption. This has the result that the most penetrating component of the photons moves near the center of the plane channel. In this region of distances, the variation of $\chi(\omega, x)$ is close to a parabola. Hence the period of oscillations of the trajectory practically does not depend on the amplitude, and hence on the entry point x_0. The independence of the period on the amplitude leads to an effect of oscillation of the angular divergence of the beam of channeled particles upon changing their depth of penetration into the target. This effect was observed earlier in the planar channeling of protons.[2]

Figure 22 shows the results[139] of measurements of the angular divergence of a beam of photons as a function of the target thickness z, confirming the oscillating character of the angular divergence. Thus one can consider that the effect of channeling of photons in superlattices has been detected experimentally. However, more favorable conditions for observing it exist in superlattices with a smaller period (~ 1 μm) and for harder quanta (~ 100 keV).

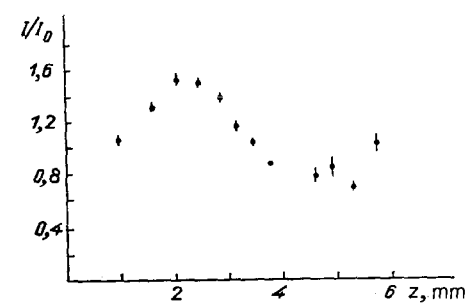

FIG. 22. Relative intensity of the radiation of the K_α line of silver scattered at zero angle in a periodic structure as a function of the target thickness z. The initial angular divergence of the beam is 0.2°, and the receiving angle of the detector is 0.03°.

CLOSING REMARKS

The process of channeling of electrons and positrons in crystals and the accompanying electromagnetic radiation has been studied at present over a broad range of energies of the channeled particles from ~ 1 MeV to ~ 100 GeV. On the whole, the theory that has been developed agrees well with the results of experiments. The effect of emission by particles of relatively low energies has already found application in solid-state physics as a new method of spectroscopy. The further prospects of this method of studying solids involve the development of a theory of the broadening of the spectral lines toward improving the accuracy of predictions of the positions and line widths of the emission with account taken of various subtle effects of interaction of the particles with the crystal lattice. As experiments have shown, the emission by particles of medium and high energies has a relatively high intensity, while the emission by positrons of energies 1–10 GeV in planar channeling has also a rather high monochromaticity (owing to the almost harmonic oscillations in the channel and the dipole character of the emission), and it can be tuned in frequency. Such a radiation source is of interest in studies of photonuclear processes. As regards the emission from channeled and superbarrier particles of superhigh ($\gtrsim 100$ GeV) energies, it is the most effective means of obtaining hard γ-quanta with energies comparable with the energy of the particles, since the probability of emission in this case is an order of magnitude higher than for bremsstrahlung in an amorphous material. From the standpoint of theory this process also arouses great interest, since under certain conditions is serves as an example of electromagnetic processes in a strong constant field. Finally we note that, owing to the lack of space, such an interesting phenomenon as the channeling of relativistic particles in bent crystals, which also has been intensively studied recently and can find widespread application in high-energy physics, has remained outside the scope of this review.

The authors thank H. F. Shul'ga, who made a number of useful comments on the manuscript of the article.

[1] J. Lindhard, Dansk. Vid. Selsk. Mat.-Fiz. Medd. **34**, 30 (1965).
[2] D. S. Gemmell, Rev. Mod. Phys. **46**, 129 (1974).
[3] R. Wedell, Phys. Status Solidi B **99**, 11 (1980).
[4] A. I. Akhiezer and N. F. Shul'ga, Usp. Fiz. Nauk **137**, 561 (1982) [Sov. Phys. Usp. **25**, 541 (1982)].
[5] V. A. Bazylev and N. K. Zhevago, *ibid.*, p. 605 [Sov. Phys. Usp. **25**, 565 (1982)].
[6] V. A. Bazylev and N. K. Zhevago, *Emission from Fast Particles in Matter and in External Fields* (in Russian), Nauka, M., 1987.
[7] F. V. Andersen and E. Laegsgaard, Phys. Rev. Lett. **44**, 1079 (1979).
[8] R. L. Swent, R. H. Pantell, M. J. Alguard *et al.*, *ibid.* **43**, 1723 (1979).
[9] V. V. Kaplin and S. A. Vorob'ev, Zh. Eksp. Teor. Fiz. **73**, 583 (1977) [Sov. Phys. JETP **46**, 304 (1977)]; Fiz. Tverd. Tela (Leningrad) **19**, 1958 (1977) [Sov. Phys. Solid State **19**, 1145 (1977)].
[10] V. A. Basylev and V. V. Goloviznin, Radiat. Eff. **60**, 101 (1982); **69**, 159 (1987).
[11] V. A. Bazylev and V. V. Goloviznin, Zh. Eksp. Teor. Fiz. **82**, 1204 (1982) [Sov. Phys. JETP **55**, 700 (1982)]; Dokl. Akad. Nauk SSSR Ser. Fiz. **266**, 1112 (1982) [Sov. Phys. Dokl. **27**, 852 (1982)].
[12] F. V. Andersen, E. Bonderup, E. Laegsgaard *et al.*, Nucl. Instrum. Methods **194**, 209 (1982).
[13] S. A. Mikheev and A. V. Tulupov, Fiz. Tverd. Tela (Leningrad) **28**, 2447 (1986) [Sov. Phys. Solid State **28**, 1368 (1986)].
[14] N. Cue, E. Bonderup, B. Marsh *et al.*, Phys. Lett. A **80**, 26 (1980).
[15] M. J. Alguard, R. L. Swent, R. H. Pantell *et al.*, Nucl. Instrum. Methods **170**, 7 (1980).
[16] B. L. Berman, S. D. Bloom, S. Datz *et al.*, Phys. Lett. A **82**, 459 (1981).
[17] F. V. Andersen, K. R. Eriksen, and E. Laegsgaard, Phys. Scripta **24**, 588 (1981).
[18] R. L. Swent, R. H. Pantell, and R. Alvares, Nucl. Instrum. Methods **194**, 235 (1982).
[19] Y. E. Watson and Y. Kochler, Phys. Rev. B **25**, 3075 (1982).
[20] Y. V. Andersen, S. Datz, E. Laegsgaard *et al.*, Phys. Rev. Lett. **49**, 215 (1982).
[21] M. Gouanere, D. Sillou, M. Spigel *et al.*, Nucl. Instrum. Methods **194**, 225 (1982).
[22] S. Datz, R. W. Fearick, H. Park *et al.*, Phys. Lett. A **96**, 314 (1983).
[23] Y. V. Andersen, E. Bonderup, E. Laegsgaard *et al.*, Phys. Scripta **28**, 308 (1983).
[24] Y. V. Andersen, E. Laegsgaard, and A. H. Sorensen, Nucl. Instrum. Methods B **230**, 63 (1984).
[25] E. Laegsgaard and Y. U. Andersen, *ibid.*, p. 99.
[26] S. Datz, R. W. Fearick, H. Park *et al.*, *ibid.*, p. 74.
[27] H. Park, R. H. Pantell, and R. L. Swent, J. Appl. Phys. **55**, 358 (1984).
[28] B. L. Berman, S. Datz, R. W. Fearick *et al.*, Nucl. Instrum. Methods B **230**, 90 (1984) [sic].
[29] R. L. Swent, R. H. Pantell, H. Park *et al.*, Phys. Rev. B **29**, 52 (1984).
[30] N. Cue, B. B. Marsh, R. E. Benenson *et al.*, Nucl. Instrum. Methods B **230**, 104 (1984).
[31] B. L. Berman, B. Dahling, S. Datz *et al.*, *ibid.* Ser. B **10/11**, 611 (1985).
[32] H. Park, Y. O. Kephart, R. K. Klein *et al.*, J. Appl. Phys. **57**, 1661 (1985).
[33] R. K. Klein, Y. O. Kephart, R. H. Pantell *et al.*, Phys. Rev. B **31**, 68 (1985).
[34] S. Datz, B. L. Berman, B. A. Dahling *et al.*, Nucl. Instrum. Methods B **13**, 19 (1986).
[35] H. Part, Y. O. Kephart, R. K. Klein *et al.*, Phys. Rev. B **35**, 13 (1987).
[36] A. A. Vorobiev, V. V. Kaplin, and S. A. Vorobiev, Nucl. Instrum. Methods **127**, 265 (1975).
[37] P. Lervig, Y. Lindhard, and V. Nielsen, Nucl. Phys. A **96**, 481 (1967).
[38] J. U. Andersen, S. K. Andersen, and K. Augustiniak, Dansk. Vid. Selsk. Mat.-Fiz. Medd. **39**, No. 10 (1977).
[39] B. R. Appleton, C. Erginsoy, and W. M. Gibson, Phys. Rev. **161**, 330 (1967).
[40] K. Kimura and M. Makhami, Phys. Lett. A **89**, 299 (1982).
[41] S. A. Mikheev and A. V. Tulupov, Fiz. Tverd. Tela (Leningrad) **29**, 449 (1987) [Sov. Phys. Solid State **29**, 256 (1987)].
[42] V. A. Bazylev and V. V. Goloviznin, Preprint IAÉ-3808-1, Moscow, 1983; Zh. Eksp. Teor. Fiz. **91**, 25 (1986) [Sov. Phys. JETP **64**, 14 (1986)].
[43] A. V. Tulupov, Fiz. Tverd. Tela (Leningrad) **23**, 46 (1981) [Sov. Phys. Solid State **23**, 25 (1981)]; Radiat. Eff. **56**, 77 (1981); Zh. Eksp. Teor. Fiz. **81**, 1639 (1981) [Sov. Phys. JETP **57**, 872 (1981)].
[44] V. A. Bazylev, S. A. Mikheev, and A. V. Tulupov, Radiat. Eff. **114**, 114 (1990).
[45] K. Komaki, F. Fujimoto, and A. Ootuka, Nucl. Instrum. Methods **194**, 243 (1982).
[46] A. V. Tulupov, Zh. Eksp. Teor. Fiz. **86**, 1365 (1984) [Sov. Phys. JETP **59**, 797 (1984)].
[47] L. V. Hau, E. Laegsgaard, and Y. U. Andersen, Preprint Inst. Phys. Aarhus, 1989.
[48] S. A. Mikheev and A. V. Tulupov, *Abstracts of the All-Union Conference on the Interaction of Charged Particles with Crystals* (in Russian). MGU, M., 1989, p. 467.
[49] B. R. Meshcherov and V. I. Tumanov, Pis'ma Zh. Eksp. Teor. Fiz. **51**, 239 (1990) [JETP Lett. **51**, 272 (1990)].
[50] A. F. Burenkov, Yu. I. Dudchik, and F. F. Komarov, Radiat. Eff. Lett. **83**, 241 (1984).
[51] V. A. Bazylev, S. A. Mikheev, and A. V. Tulupov, Fiz. Tverd. Tela (Leningrad) **30**, 2445 (1988) [Sov. Phys. Solid State **30**, 1409 (1988)].
[52] B. A. Gurskiĭ and Z. A. Gurskiĭ, Usp. Fiz. Nauk **21**, 1603 (1976); **23**, 19 (1978) [sic].
[53] S. A. Mikheev and A. V. Tulupov, Fiz. Tverd. Tela (Leningrad) **27**, 1307 (1985) [Sov. Phys. Solid State **27**, 791 (1985)].
[54] V. A. Bazylev and N. K. Zhevago, *Proc. 7th Intern. Conference on Atomic Collisions in Solids,* Moscow, Sep. 19–23, 1977; Preliminary Programme and Abstracts of Papers, Pt. I, Moscow State University Publ. House, Moscow, 1977, p. 65.
[55] G. Moliere, Z. Naturforsch. **2a**, 133 (1947).
[56] P. A. Doyle and R. S. Turner, Acta Crystallogr. Sect. A **24**, 390 (1968).
[57] N. F. M. Henry and K. Lonsdale, eds., International Tables for X-Ray Crystallography, Kynoch, Birmingham, 1959.
[58] V. I. Glebov, V. V. Goloviznin, and A. M. Kanloev, Preprint IAÉ-3905-1, Moscow, 1984, p. 36.; A. R. Avakian, V. I. Glebov, V. V. Goloviznin *et al.*, Radiat. Eff. **80**, 14 (1984).
[59] R. Rabe, G. Tolkiehn, and A. Werner, J. Phys. C **12**, 1545 (1979).
[60] W. Bohmer and P. Rabe, *ibid.*, p. 2465.
[61] R. I. Glauber, Phys. Rev. **98**, 1692 (1955).
[62] D. P. Jackson, B. M. Powell, and G. Dolling, Phys. Lett. A **51**, 87 (1975).

[63] O. H. Nielsen and W. Weber, J. Phys. C **13**, 2449 (1980).
[64] N. F. Shul'ga, V. I. Truten', and S. P. Fomin, Zh. Eksp. Teor. Fiz. **87**, 250 (1984) [Sov. Phys. JETP **60**, 145 (1984)].
[65] S. P. Fomin and N. F. Shulga, Phys. Lett. A **73**, 131 (1979).
[66] N. F. Shul'ga, V. I. Truten', and S. P. Fomin, Zh. Tekh. Fiz. **52**, 2279 (1982) [Sov. Phys. Tech. Phys. **27**, 1399 (1982)].
[67] N. F. Shulga, V. I. Truten', and S. P. Fomin, Radiat. Eff. **84**, 182 (1985).
[68] N. K. Bulgakov, A. S. Vodop'yanov, V. M. Golovatyuk *et al.*, JINR Preprint 1-83-640, Dubna, 1983.
[69] S. K. Andersen, O. Fish, and I. A. Golovchenko, Nucl. Phys. B **167**, 1 (1980).
[70] V. A. Bazylev, V. V. Goloviznin, and A. V. Demura, Zh. Eksp. Teor. Fiz. **92**, 1946 (1987) [Sov. Phys. JETP **65**, 1093 (1987)].
[71] V. A. Bazylev, V. I. Glebov, and V. V. Goloviznin, *ibid.* **91**, 25 (1986) [Sov. Phys. JETP **64**, 14 (1986)].
[72] Yu. V. Martynenko, Fiz. Tverd. Tela (Leningrad) **13**, 1055, 2580 (1971) [Sov. Phys. Solid State **13**, 876 (1971), 2166 (1972)].
[73] E. Bonderup, H. Esbensen, and I. U. Andersen, Radiat. Eff. **12**, 261 (1972).
[74] V. V. Beloshitskiĭ and M. A. Kumakhov, Zh. Eksp. Teor. Fiz. **62**, 1144 (1972) [Sov. Phys. JETP **35**, 605 (1972)].
[75] V. A. Bazylev, V. I. Glebov, and V. V. Goloviznin, Dokl. Akad. Nauk SSSR **288**, 105 (1986) [Sov. Phys. Dokl. **31**, 410 (1986)].
[76] A. I. Akhiezer and N. F. Shul'ga, Usp. Fiz. Nauk **151**, 385 (1987) [Sov. Phys. Usp. **30**, 197 (1987)].
[77] G. M. Zaslavskiĭ, *Stochasticity of Dynamic Systems* (in Russian), Nauka, M., 1984.
[78] B. V. Chirikov, Phys. Rep. **52**, 263 (1979).
[79] G. I. Budker and S. T. Belyaev, *Plasma Physics and Problems of Controlled Thermonuclear Reactions*, Vol. 2 (in Russian), Atomizdat, M., 1958.
[80] V. A. Bazylev and N. K. Zhevago, Zh. Eksp. Teor. Fiz. **77**, 1267 (1979) [Sov. Phys. JETP **50**, 637 (1979)]; Radiat. Eff. **54**, 221 (1981).
[81] A. G. Bonch-Osmolovskiĭ and M. I. Podgoretskiĭ, Yad. Fiz. **29**, 432 (1979) [Sov. J. Nucl. Phys. **29**, 216 (1979)].
[82] V. G. Baryshevskiĭ, *Channeling, Emission, and Reactions in Crystals at High Energies* (in Russian), Izd-vo Bel. Un-ta, Minsk, 1982.
[83] V. N. Baĭer, V. M. Katkov, and V. M. Strakhovenko, Preprint of the IYaF SO AN SSSR 84-11, Novosibirsk, 1984.
[84] V. A. Bazylev and V. V. Goloviznin, Preprint of the IAÉ 4518/1, Moscow, 1987; Dokl. Akad. Nauk SSSR **293**, 1642 (1987).
[85] S. A. Vorob'ev, B. N. Kalinin, A. A. Kurkov *et al.*, *ibid.* **290**, 1252 (1986).
[86] V. L. Morokhovskiĭ and V. I. Shramenko, *Proceedings of the All-Union Conference on the Physics of Interaction of Charged Particles with Crystals* (in Russian), Izd-vo Mosk. Un-ta, M., 1976, p. 173.
[87] V. B. Ganenko, N. N. Nasonov, E. V. Pegushin *et al.*, Fiz. Elem. Chastits At. Yadra **3**, 47 (1983); V. B. Ganenko, V. I. Noga, E. V. Pegushin *et al.*, Radiat. Eff. **81**, 313 (1986); V. I. Kasilov, N. I. Lapin, V. I. Truten', and N. F. Shul'ga, Zh. Eksp. Teor. Fiz. **96**, 1927 (1989) [Sov. Phys. JETP **69**, 1086 (1989)].
[88] N. K. Zhevago, Zh. Eksp. Teor. Fiz. **75**, 1389 (1978) [Sov. Phys. JETP **48**, 701 (1978)].
[89] N. F. Shul'ga, Pis'ma Zh. Eksp. Teor. Fiz. **32**, 179 (1980) [JETP Lett. **32**, 166 (1980)].
[90] A. I. Avakian, C. Yang, and N. K. Zhevago, Radiat. Eff. **56**, 39 (1981).
[91] V. G. Baryshevski and V. V. Tikhomirov, Phys. Lett. A **90**, 153 (1982).
[92] F. C. Kimball and N. Cue, Nucl. Instrum. Methods B **230**, No. 2, 25 (1984).
[93] V. N. Baier, V. M. Katkov, and V. M. Strakhovenko, Phys. Lett. A **104**, 231 (1984).
[94] A. H. Sorensen, E. Uggerhoj, J. Bak *et al.*, Phys. Scripta **32**, 149 (1985).
[95] L. D. Landau and E. M. Lifshitz, *The Classical Theory of Fields*, 3rd ed., Pergamon Press, Oxford, 1971.
[96] A. L. Avakyan, N. K. Zhevago, and Yan Shi, Zh. Eksp. Teor. Fiz. **82**, 584 (1982) [Sov. Phys. JETP **55**, 341 (1982)].
[97] V. B. Berestetskiĭ, E. M. Lifshitz, and L. P. Pitaevskiĭ, Relativistic Quantum Theory, Part 1 Pergamon Press, Oxford, 1971).
[98] A. Belkacem, G. Bologna, M. Chevallier *et al.*, Phys. Lett. B **177**, 211 (1986).
[99] A. S. Arytyunyan, N. K. Zhevago, and Yan Shi, Izv. Akad. Nauk Arm. SSR **20**, 252 (1985).
[100] A. Belkacem, G. Bologna, M. Chevallier *et al.*, Nucl. Instrum. Methods B **33**, 1 (1988).
[101] A. Belkacem, G. Bologna, M. Chevallier *et al.*, Phys. Rev. Lett. **58**, 1196 (1987).
[102] G. Diambrini-Pallazzi, Rev. Mod. Phys. **40**, 611 (1968).
[103] M. L. Ter-Mikaelyan, *Influence of the Medium on Electromagnetic Processes at High Energies* (in Russian), Izd-vo Akad. Nauk Arm. SSR, Erevan, 1969.
[104] V. N. Baĭer, V. M. Katkov, and V. M. Strakhovenko, Zh. Eksp. Teor. Fiz. **90**, 801 (1986); **92**, 1228 (1987) [Sov. Phys. JETP **63**, 467 (1986); **65**, 686 (1987)].
[105] A. Belkacem, N. Cue, and J. C. Kimball, Phys. Lett. A **111**, 86 (1985).
[106] N. K. Zhevago, Zh. Eksp. Teor. Fiz. **94**, 23 (1988) [Sov. Phys. JETP **67**, 16 (1988)].
[107] P. Pieranski, Contemp. Phys. **24**, 25 (1983).
[108] V. A. Bazylev, V. I. Glebov, and N. K. Zhevago, Zh. Eksp. Teor. Fiz. **78**, 62 (1980) [Sov. Phys. JETP **51**, 31 (1980)].
[109] V. A. Bazylev and A. V. Demura, Radiat. Eff. **61**, 129 (1982).
[110] N. N. Nasonov, Pis'ma Zh. Tekh. Fiz. **5**, 982 (1979) [Sov. Tech. Phys. Lett. **5**, 409 (1979)].
[111] V. L. Vinetskiĭ and M. I. Faĭngol'd, Ukr. Fiz. Zh. **25**, 1093 (1980); **27**, 884 (1982); **29**, 1628 (1984).
[112] V. L. Vinetsky and M. I. Faingold, Solid State Commun. **40**, 7 (1981).
[113] N. N. Nasonov, Voprosy Atomnoĭ Nauka i Tekhniki Ser. Fizika Radiatsionnykh Povrezhdeniĭ i Radiatsionnoe Materialovedenie **3**, 85 (1982).
[114] F. F. Komarov, M. A. Kumakhov, and N. K. Zhevago, Radiat. Eff. Lett. **76**, 119 (1983).
[115] N. K. Zhevago, Dokl. Akad. Nauk SSSR **281**, 67 (1985) [Sov. Phys. Dokl. **30**, 225 (1985)].
[116] N. K. Zhevago and A. I. Ryazanov, Fiz. Tverd. Tela (Leningrad) **28**, 130 (1986) [Sov. Phys. Solid State **28**, 70 (1986); Dokl. Akad. Nauk SSSR **280**, 347 (1986) [Sov. Phys. Dokl. **30**, 61 (1986)].
[117] N. K. Zhevago and A. I. Ryazanov, Radiat. Eff. **104**, 87 (1987).
[118] V. I. Vysotskiĭ and R. N. Kuz'min, Zh. Eksp. Teor. Fiz. **79**, 481 (1980) [Sov. Phys. JETP **52**, 242 (1980)].
[119] I. I. Gurevich and L. V. Tarasov, *Physics of Low-Energy Neutrons* (in Russian), Nauka, M., 1965.
[120] H. Maier-Leibnitz and T. Springer, Nucl. Energy Ser. A/B **17**, 217 (1963).
[121] D. Mosher and S. Stephanakis, Appl. Phys. Lett. **29**, 105 (1976).
[122] W. T. Vetterling and R. V. Pound, J. Opt. Soc. Am. **66**, 1048 (1976).
[123] P. J. Malozzi, H. M. Epstein, and R. G. Jung, Appl. Phys. **45**, 1891 (1974).
[124] A. Rindby, Nucl. Instrum. Methods A **249**, 536 (1986).
[125] G. Schmall and D. Rudolph, eds., X-Ray Optics and Microscopy [Russian Transl.], Mir, M., 1987.
[126] M. Watanabe, T. Hidaka, H. Tanino *et al.*, Appl. Phys. Lett. **45**, 725 (1984).
[127] L. D. Landau and E. M. Lifshitz, *Electrodynamics of Continuous Media*) Pergamon Press, Oxford, 1960.
[128] B. L. Henke, Atomic Data **27**, 3 (1982).
[129] A. M. Saxena and B. P. Schoenborn, Acta Crystallogr. Sect. A **33A**, 805 (1977).
[130] K. Krishnan, Radiat. Eff. **66**, 121 (1982).
[131] E. Johnson and L. T. Chadderton, *ibid.* **79**, 183 (1983).
[132] Z. G. Pinsker, *Dynamical Scattering of X-Rays in Crystals* (in Russian), Nauka, M., 1984.
[133] E. A. Monroe, D. B. Sass, and S. H. Cole, Acta Crystallogr. Sect. A **25**, 578 (1969).
[134] J. Stone, Appl. Phys. Lett. **20**, 239 (1972).
[135] J. Schwinger, Proc. Natl. Acad. Sci. USA **40**, 132 (1954).
[136] V. N. Baĭer, V. M. Katkov, and V. S. Fadin, *Emission from Relativistic Electrons* (in Russian), Atomizdat, M., 1973.
[137] V. G. Bagrov, V. V. Belov, and V. P. Maslov, Dokl. Akad. Nauk SSSR **308**, 88 (1989) [Sov. Phys. Dokl. **34**, 809 (1989)].
[138] A. I. Akhiezer, N. V. Laskin, and N. F. Shul'ga, *ibid.* **303**, 78 (1988) [Sov. Phys. Dokl. **33**, 817 (1988)].
[139] V. I. Glebov, É. I. Denisov, and N. K. Zhevago, Fiz. Tverd. Tela (Leningrad) **31**, 275 (1989) [Sov. Phys. Solid State **31**, 151 (1989)].
[140] L. I. Ognev, Usp. Fiz. Nauk **154**, 691 (1988) [Sov. Phys. Usp. **31**, 372 (1988)].
[141] V. N. Baĭer, V. M. Katkov, and V. M. Strakhovenko, *ibid.* **159**, 455 (1989) [Sov. Phys. Usp. **32**, 972 (1989)].
[142] V. G. Baryshevskiĭ and V. V. Tikhomirov, *ibid.*, p. 529 [Sov. Phys. Usp. **32**, 1013 (1989)].
[143] B. I. Barts and N. A. Shlyakhov, Preprint of the KhFTI 88-50, TsNIIatominform, M., 1988.
[144] B. I. Barts, N. A. Shlyakhov, and N. F. Shul'ga, Zh. Eksp. Teor. Fiz. **95**, 1485 (1989) [Sov. Phys. JETP **68**, 857 (1989)].
[145] V. S. Malyshevskiĭ, V. I. Truten', and N. F. Shul'ga, Zh. Eksp. Teor. Fiz. **93**, 570 (1987) [Sov. Phys. JETP **66**, 324 (1987)].
[146] X. Artru, Nucl. Instrum. Methods B **48**, 278 (1990).
[147] Yu. V. Kononetz and V. A. Ryabov, *ibid.*, p. 289.

Translated by M. V. King